To the Graduate Council:

I am submitting herewith a thesis written by Nancy Lee Copeland Johnson entitled "Transition Metal Methanesulfonates and Hypophosphites." I recommend that it be accepted in partial fulfillment of the requirements for the degree of Master of Science, with a major in Chemistry.

William E Bull
William E. Bull, Major Professor

We have read this thesis
and recommend its acceptance:

Geo. K. Schweitzer

James Q. Chambers

Accepted for the Council:

L Evans Roth
Vice Chancellor
Graduate Studies and Research

TRANSITION METAL METHANESULFONATES AND HYPOPHOSPHITES

A Thesis

Presented for the

Master of Science

Degree

The University of Tennessee, Knoxville

by

Nancy Lee Copeland Johnson

June 1977

1324061

ACKNOWLEDGMENTS

The author wishes to express her gratitude to Dr. William E. Bull for his guidance, patience, and encouragement during the course of this work.

The author wishes to thank her husband, Randy, for his continuous encouragement.

The author is indebted to Mr. Ray Hinton for performing the far-infrared measurements. Thanks are also due to Mrs. Joyce Wallace for the typing and to Mr. Bernard Cox for sketching the spectra.

ABSTRACT

Two series of compounds were prepared. The first has the general formula $[ML_4(CH_3SO_3)_2]$ where M represents divalent cobalt, nickel, or copper, and L represents pyridine or 4-methylpyridine. The second group of compounds contains the anhydrous cobalt(II) and nickel(II) hypophosphites. Also prepared were $[Co(py)_2(CH_3SO_3)_2]$ and $[Ni(py)_2(H_2PO_2)_2]$.

The compounds were characterized by visible and infrared spectroscopy and magnetic susceptibilities.

These measurements are consistent with monodentate coordination of the methanesulfonate anion in tetragonally distorted octahedral $[ML_4(CH_3SO_3)_2]$ complexes.

Anion coordination in anhydrous $Co(H_2PO_2)_2$ and $Ni(H_2PO_2)_2$ and in $[Ni(py)_2(H_2PO_2)_2]$ and in $[Co(py)_2(CH_3SO_3)_2]$ is proposed to be as bridging and chelating bidentate ligands. Tetragonal distortion is small for these compounds.

The electronic spectral parameters Ds, Dt, Dq_{xy}, and Dq_z were calculated from visible and near-infrared spectral data for the $[NiL_4(CH_3SO_3)_2]$ complexes. These calculations indicate that the methanesulfonate anion coordinates more strongly than ClO_4^- and BF_4^- but less strongly than Cl^- and Br^-.

TABLE OF CONTENTS

CHAPTER		PAGE
I.	INTRODUCTION	1
II.	EXPERIMENTAL	5
	A. Reagents	5
	1. Hydrated cobalt(II), nickel(II), and copper(II) methanesulfonates	5
	2. Pyridine Bases	5
	3. Hypophosphorous acid	5
	4. Hydrated cobalt(II) and nickel(II) benzoates	6
	5. Other reagents	6
	B. Syntheses and Analytical Results	6
	1. Methanesulfonate complexes	6
	2. Hypophosphite compounds	7
	C. Analytical Data	12
	D. Magnetic Susceptibility	12
	E. Infrared Spectroscopy	14
	F. Visible and Near-Infrared Spectroscopy	14
III.	RESULTS AND DISCUSSION	16
	A. General Properties	16
	B. Magnetic Susceptibilities	16
	C. Infrared Spectra	18
	1. Methanesulfonate bands	18
	2. Hypophosphite bands	25
	3. Pyridine bands	34

CHAPTER PAGE

4. Metal-ligand bands 35

D. Visible and Near-Infrared Spectra 39

1. Introduction 39

2. Cobalt(II) spectra 41

3. Nickel(II) spectra 50

4. Copper(II) spectra 60

IV. SUMMARY 67

LIST OF REFERENCES 69

APPENDIX 74

VITA 78

LIST OF TABLES

TABLE		PAGE
I.	Methanesulfonate Complexes — Analytical Data and Melting Points	8
II.	Anhydrous Hypophosphites — Analytical Data and Decomposition Temperatures	11
III.	Magnetic Susceptibilities	17
IV.	Infrared Absorptions (cm^{-1}) of Ionic and Coordinated CH_3SO_3 Groups	19
V.	CH_3SO_3 Vibrational Frequencies (cm^{-1}) in Complexes	21
VI.	Infrared Absorptions (cm^{-1}) of Ionic and Coordinated H_2PO_2 Groups	26
VII.	Hypophosphite Vibrations in Anhydrous Compounds (cm^{-1})	30
VIII.	Infrared Absorptions of Free and Coordinated Pyridine and 4-Methylpyridine	36
IX.	Infrared Absorptions of Metal-Ligand Vibrations (cm^{-1})	38
X.	Electronic Spectral Data for Cobalt(II) Compounds	46
XI.	Electronic Spectral Data for $[NiL_4(CH_3SO_3)_2]$ (cm^{-1})	55
XII.	Electronic Spectral Parameters for $[NiL_4(CH_3SO_3)_2]$ (cm^{-1})	57
XIII.	Electronic Spectral Data for $Ni(H_2PO_2)_2$ and $[Ni(py)_2(H_2PO_2)_2]$	61
XIV.	Electronic Absorption Bands for Copper(II) Complexes	65

LIST OF FIGURES

FIGURE		PAGE
1.	Infrared Spectrum of $[Co(py)_4(CH_3SO_3)_2]$	22
2.	Infrared Spectrum of $[Cu(4\text{-mepy})_4(CH_3SO_3)_2]$	23
3.	Infrared Spectrum of $Co(H_2PO_2)_2$	31
4.	Infrared Spectrum of $Ni(H_2PO_2)_2$	32
5.	Splitting of 3d Orbitals in Octahedral and Tetragonally Distorted Octahedral Fields	40
6.	Splitting of the ^4P and ^4F States of Cobalt(II) in An Octahedral Crystal Field	42
7.	Visible and Near-Infrared Spectra of $[Co(py)_4(CH_3SO_3)_2]$ As A Nujol Mull (Dotted Line) and As A Dichloromethane Solution (Solid Line)	44
8.	Visible and Near-Infrared Spectra of $[Co(4\text{-mepy})_4(CH_3SO_3)_2]$ As A Nujol Mull (Dotted Line) and As A Dichloromethane Solution (Solid Line)	45
9.	Visible and Near-Infrared Spectrum of $[Co(py)_2(CH_3SO_3)_2]$ As A Nujol Mull	47
10.	Visible and Near-Infrared Spectrum of $Co(H_2PO_2)_2$ As A Nujol Mull	49
11.	Correlation Diagram for A d^8 Configuration in Crystal Fields of O_h and D_{4h} Symmetry	51
12.	Visible and Near-Infrared Spectra of $[Ni(py)_4(CH_3SO_3)_2]$ As A Nujol Mull (Dotted Line) and As A Dichloromethane Solution (Solid Line)	52

FIGURE PAGE

13. Visible and Near-Infrared Spectra of $[Ni(4\text{-mepy})_4(CH_3SO_3)_2]$ As A Nujol Mull (Dotted Line) and As A Dichloromethane Solution (Solid Line) 53

14. Visible and Near-Infrared Spectrum of $Ni(H_2PO_2)_2$ As A Nujol Mull 59

15. Visible and Near-Infrared Spectrum of $[Ni(py)_2(H_2PO_2)_2]$ As A Nujol Mull 62

16. Splitting of the ^2D Spectroscopic Term for Copper(II) in Octahedral and Tetragonally Distorted Octahedral Fields . 64

17. Visible and Near-Infrared Spectra of $[Cu(4\text{-mepy})_4(CH_3SO_3)_2]$ As A Nujol Mull (Dotted Line) and As A Dichloromethane Solution (Solid Line) 66

18. Splitting of the d Orbitals in Crystal Fields of O_h and D_{4h} Symmetry 76

CHAPTER I

INTRODUCTION

Methanesulfonic acid is a strong (K_a,4)[1] monobasic acid. It is ranked stronger than nitric and phosphoric acids but not as strong as sulfuric acid.[1-4] As the anion of a strong acid, the methanesulfonate group would be expected to coordinate only weakly to metal ions in complex compounds; relatively little, however, is known about the coordinating properties of this group.

Paul and coworkers[5] have reported the synthesis and characterization of anhydrous cobalt(II), nickel(II), copper(II), vanadium(III), and chromium(III) methanesulfonates. These compounds were found to be high-spin octahedral complexes. A polymeric structure was proposed. From the electronic spectrum of nickel(II) methanesulfonate, ligand field parameters were evaluated.

Yeats, Sams, and Aubke[6] synthesized trimethyltin(IV) methanesulfonate by acid solvolysis of $(CH_3)_4Sn$ in a one-step procedure. The presence of bridging CH_3SO_3 groups was indicated by infrared and ^{119}Sn Mössbauer spectra, suggesting a polymeric structure with pentacoordination about the tin(IV).

Infrared and Raman[2,7-13] studies of methanesulfonic acid and its salts and esters have indicated local C_s symmetry about the sulfur atom for the acid, esters, and the lithium salt. The methanesulfonate anion has been found to possess C_{3v} symmetry in the ammonium, potassium, and sodium salts. A normal coordinate analysis was performed on the anion by Fujimori.[14]

The coordinating properties of anions of strong acids have been the subject of several studies. In particular, the anions of perchloric,[15-17] tetrafluoroboric,[17-19] hexafluorophosphoric,[20] and trifluoromethanesulfonic[21] acids have been extensively investigated in the last fifteen years. A review of the coordinating tendencies of anions of strong acids has been presented by Rosenthal.[22]

Preliminary studies of Turk, Mayfield, and Bull[23] have shown promise of providing data such that the methanesulfonate anion could be placed in the spectrochemical series along with BF_4^-, ClO_4^-, PF_6^-, and anions of other strong acids. Therefore, cobalt(II), nickel(II), and copper(II) methanesulfonate complexes containing pyridine and 4-methylpyridine were chosen for study.

Like methanesulfonic acid, hypophosphorous acid, H_3PO_2, is a strong monobasic acid (K_a, 0.06)[24] which reacts readily with most metal oxides, hydroxides, and carbonates to form hypophosphite salts. In cases where the metal ion can be readily reduced, for example copper(II), a redox reaction occurs instead of salt formation.[25]

Lovejoy and Wagner[26] have obtained the infrared spectrum of hypophosphorous acid at liquid air temperature. The spectrum was assigned on the basis of C_1 symmetry, and a structure was postulated where the individual acid molecules are held together in a crystalline aggregate by strong hydrogen bonds.

The structure of the hypophosphite anion has been shown by X-ray diffraction of the ammonium salt to be a distorted tetrahedron with oxygen atoms at two of the corners, hydrogen atoms at the other two corners, and the phosphorus atom at the tetrahedral center.[27]

Raman and infrared studies[26,28,29] of hypophosphite salts have indicated C_{2v} symmetry for the anion, except for the calcium salt where the H_2PO_2 group displays C_1 symmetry.

Mayants and Matrosov[30] studied the infrared spectra of many metal hypophosphites in order to determine the influence of the metal on polymeric properties of the anion. It was concluded that salts of the alkali and alkaline earth metals are ionic to a considerable degree and the hypophosphite ion is well represented by a model with equalized PO bond lengths. For salts of nonionic structure (e.g., bivalent cobalt, lead, zinc, and manganese hypophosphites), a chain model with equalized PO bond distances was proposed. In this model the metal ion is bonded to one oxygen atom of each anion; a coordination number of four was assumed.

Brun and Dumail[25] have reported the preparation of anhydrous iron(II), nickel(II), cobalt(II), and zinc(II) hypophosphites. The cobalt(II) and zinc(II) salts were crystallized from a warm (30°C) aqueous solution; the hexahydrates crystallized around 20°C. $Fe(H_2PO_2)_2$ and $Ni(H_2PO_2)_2$ were precipitated from acetone and the nickel(II) salt was dried over P_4O_{10}. X-ray diffraction patterns were obtained for these compounds.

Upon stirring the anhydrous hypophosphites in pyridine,[25] the iron and nickel compounds underwent self-oxidation-reduction. The cobalt(II) and zinc(II) hypophosphites, however, combined with pyridine(py) to give $Co(H_2PO_2)_2py_2$ and $Zn(H_2PO_2)_2py_2$. These compounds slowly lost pyridine at room temperature. Brun and Dumail concluded from infrared data that the hypophosphite anion was coordinated to the

metal in the pyridine compounds and in the anhydrous salts, but not in the hexahydrates. They were unable to determine whether the hypophosphite ion was monodentate or bidentate.

A literature search has revealed a number of detailed infrared and Raman spectral studies of metal hypophosphites;[25-34] however, other methods of characterization have received little attention. Brun and Dumail[25] reported syntheses, yet neither elemental analysis nor infrared spectral data in the regions of water absorption were presented. Mayants and Matrosov[30] observed that drying the salts over P_4O_{10} at 77°C led to only partial loss of water of crystallization. Therefore, it seemed desirable to prepare and study several anhydrous hypophosphite compounds. Cobalt(II) and nickel(II) hypophosphites along with their bispyridine complexes were chosen for study.

Infrared and electronic spectroscopy plus magnetic susceptibility measurements were primary tools for structural elucidation.

CHAPTER II

EXPERIMENTAL

A. Reagents

1. Hydrated Cobalt(II), Nickel(II), and Copper(II) Methanesulfonates

The hydrated cobalt(II), nickel(II), and copper(II) methanesulfonates were prepared by treating an excess of the metal carbonate with methanesulfonic acid. The excess carbonate was removed by filtration and the filtrate evaporated until crystals formed. The crystals were dried at 78°C for several days.

2. Pyridine Bases

ACS grade pyridine(py) was used as received from Fisher Scientific Co. Reagent grade 4-methylpyridine(4-mepy) was supplied by Eastman Organic Chemicals and was redistilled once (b.p. 143-5°C).

3. Hypophosphorous Acid

Fisher Scientific Company was the source of a 50 per cent aqueous solution of hypophosphorous acid. Because the commerical grade acid usually contains a small amount of phosphorous acid[35] it seemed worthwhile to carry out iodometric titrations[36] on the acid as received. It was determined that the phosphite ion concentration was no greater than 5 mole per cent and could be ignored for this work.

Anhydrous hypophosphorous acid was prepared by refluxing the aqueous acid solution with an excess of benzene for 30 minutes. The benzene-water azeotrope was then removed by distillation. This procedure was repeated a second time to ensure complete removal of water.

The temperature of the liquid in the pot could not be allowed to exceed 100°C or hypophosphorous acid would undergo decomposition to phosphine and phosphorous acid.

4. Hydrated Cobalt(II) and Nickel(II) Benzoates

An aqueous solution of hydrated metal(II) chloride (0.17 mole, approximately 40 grams) was added to an aqueous solution of sodium benzoate (0.34 mole, 48 grams). The immediately precipitated metal(II) benzoate was suction filtered and washed twice with distilled water. It was dried at 78°C for three days.

5. Other Reagents

Cobalt(II), nickel(II), and copper(II) carbonates and chlorides were used as received from J. T. Baker Chemical Company. Sodium benzoate was supplied by Merck and Co., Inc.

Practical grade methanesulfonic acid was supplied by Eastman Organic Chemicals. Qualitative tests were made to determine whether the acid was contaminated with sulfate or chloride ions — both tests were negative.

Methanol, anhydrous ethyl ether, and benzene were supplied by Fisher Scientific Co. Practical grade 2,2-dimethoxypropane (DMP) and spectral grade dichloromethane were obtained from Eastman Organic Chemicals.

B. Syntheses and Analytical Results

1. Methanesulfonate Complexes

a. Tetrapyridine complexes. All the methanesulfonate complexes were prepared in the same general manner. Approximately 2 grams

(8×10^{-3} mole) of the hydrated metal(II) methanesulfonate was dissolved in a minimal amount of methanol and 2,2-dimethoxypropane (DMP). The solution was stirred for one hour, after which an excess of pyridine or 4-methylpyridine (5×10^{-2} mole, approximately 5 ml) was slowly added with stirring. If the complex did not precipitate within 30 minutes, anhydrous ether was added dropwise to force precipitation. Each complex was filtered in a nitrogen atmosphere, dried at 65°C under reduced pressure for several hours, and stored in the dry box.

Table I summarizes the analytical data and melting points for the $[ML_4(CH_3SO_3)_2]$ complexes.

b. Bismethanesulfonatobispyridinecobalt(II), $[Co(py)_2(CH_3SO_3)_2]$. Pink bismethanesulfonatotetrapyridinecobalt(II), $[Co(py)_4(CH_3SO_3)_2]$, was heated at 110°C in an Abderhalden pistol until a uniform purple product was obtained. It decomposes at temperatures above 250°C. Analytical data are presented in Table I.

2. Hypophosphite Compounds

a. Anhydrous cobalt(II) and nickel(II) hypophosphites. Two synthetic routes were employed to prepare nearly anhydrous cobalt(II) and nickel(II) hypophosphites. The first procedure involved formation of the hydrated salt and its subsequent dehydration by stirring with 2,2-dimethoxypropane.

A dilute solution of hypophosphorous acid (9×10^{-2} mole, 10 ml of the 50 per cent acid solution diluted to 100 ml volume) was added slowly and with stirring to an aqueous slurry of the metal carbonate

TABLE I

METHANESULFONATE COMPLEXES — ANALYTICAL DATA AND MELTING POINTS[a]

Complex	Color	Mp, °C	Elemental Analyses, Calculated (Found), % C	H	N
$[Co(py)_2(CH_3SO_3)_2]$	Purple	250	35.38 (35.77)	3.97 (4.29)	6.88 (7.05)
$[Co(py)_4(CH_3SO_3)_2]$	Pink	200[a]	46.72 (46.63)	4.64 (4.74)	9.91 (9.87)
$[Ni(py)_4(CH_3SO_3)_2]$	Blue	180[a]	46.74 (46.61)	4.65 (4.69)	9.91 (9.84)
$[Cu(py)_4(CH_3SO_3)_2]$	Dark Blue	190	46.34 (46.09)	4.61 (4.72)	9.82 (9.70)
$[Co(4\text{-mepy})_4(CH_3SO_3)_2]$	Pink	195-8	50.23 (50.30)	5.52 (5.44)	9.02 (8.97)
$[Ni(4\text{-mepy})_4(CH_3SO_3)_2]$	Blue	215-7	50.25 (48.65)	5.52 (5.26)	9.02 (7.73)
$[Cu(4\text{-mepy})_4(CH_3SO_3)_2]$	Dark Blue	173-5	49.86 (50.30)	5.47 (5.21)	8.95 (7.88)

[a]Decomposition temperature.

(6×10^{-2} mole, approximately 7 grams). To prevent reduction of cobalt(II) to the metal, it was necessary that the carbonate be in excess and that the system be cooled in an ice bath as the reaction proceeded. These precautions were not required for nickel(II).

Stirring was continued for two hours to ensure complete reaction. Excess carbonate was removed by filtration and the solution was partially evaporated at room temperature to induce crystallization. The hydrated salt was oven dried at 78°C for several days. Some water of hydration appeared to be lost during the drying as evidenced by color changes: pink $Co(H_2PO_2)_2 \cdot 6H_2O$ became purple when heated, whereas green $Ni(H_2PO_2)_2 \cdot 6H_2O$ turned chartreuse on heating.

The partially dehydrated metal(II) hypophosphites were insoluble in methanol, ethanol, isopropyl alcohol, acetonitrile, nitromethane, dichloromethane, and tetrahydrofuran; they dissolved readily in water.

Complete dehydration was attempted by stirring the metal hypophosphite in methanol containing a small amount of DMP (50 ml to 3 ml) for four hours. DMP is a dehydrating agent which reacts with water in hydrated metal salts to form acetone and methanol.[37] The slurry was then filtered and the recovered solid stirred with fresh methanol and DMP for another hour, after which it was filtered and washed with anhydrous ether in a nitrogen atmosphere in the dry box. For approximately 12 hours, the solid was dried at 100°C under reduced pressure in an Abderhalden drying pistol.

$Co(H_2PO_2)_2$ remained purple as it underwent nearly complete dehydration; $Ni(H_2PO_2)_2$ became a brilliant yellow as it lost water of hydration.

The second method for preparing nearly anhydrous cobalt(II) and nickel(II) hypophosphites was based on that used by Alleyne et al. for the synthesis is bisfluorosulfates.[38] To a saturated solution of metal benzoate (3×10^{-2} mole, approximately 9 grams) in methanol and dimethoxypropane (50 ml: 3 ml), a large excess of anhydrous acid was added. Purple cobalt(II) hypophosphite precipitated immediately; addition of almost one pint of ether was required to force yellow $Ni(H_2PO_2)_2$ out of solution. The product was filtered and washed with ether in the dry box and then dried for four hours at 100°C at reduced pressure.

Table II presents analytical data and decomposition temperatures for the hypophosphites.

The author was unable to repeat the results of Brun and Dumail[25] to obtain anhydrous cobalt(II) and nickel(II) hypophosphites. Considerable absorption due to OH stretching and bending was indicated in the infrared spectra of the compounds prepared by their procedures.

b. Dihypophosphitobispyridinenickel(II), $[Ni(py)_2(H_2PO_2)_2]$. Hydrated nickel hypophosphite (7×10^{-2} mole, approximately 2 grams) was stirred in 10 ml methanol plus 10 ml dimethoxypropane for several hours. Pyridine was added dropwise until all the hydrated $Ni(H_2PO_2)_2$ dissolved producing a blue solution. Upon addition of ether, an oil formed; tituration of the oil with ether produced a green solid. This product was dried at 65°C under reduced pressure for 12 hours. It decomposes at 130°C. Anal. Calcd. for $[Ni(py)_2(H_2PO_2)_2]$: C, 34.62; H, 4.07; N, 8.08. Found: C, 34.43; H, 4.13; N, 7.96.

TABLE II

ANHYDROUS HYPOPHOSPHITES — ANALYTICAL DATA AND DECOMPOSITION TEMPERATURES

Compound	Preparation Method	Decomposition Temperature °C	Elemental Analysis % H
$Co(H_2PO_2)_2$	Dehydration	220	2.37
$Co(H_2PO_2)_2$	Benzoate-acid	220	2.27
$Co(H_2PO_2)_2$ (Calculated)	---	---	2.13
$Co(H_2PO_2)_2 \cdot H_2O$ (Calculated)	---	---	2.92
$Ni(H_2PO_2)_2$	Dehydration	225	2.52
$Ni(H_2PO_2)_2$	Benzoate-acid	205	2.83
$Ni(H_2PO_2)_2$ (Calculated)	---	---	2.14
$Ni(H_2PO_2)_2 \cdot H_2O$ (Calculated)	---	---	2.93

c. Attempted preparation of $[Co(py)_2(H_2PO_2)_2]$. The same procedure as for the analogous Ni(II) compound was followed for this synthesis. Elemental analysis indicated that a badly defined mixture of pyridine complexes formed. Anal. Calcd. for $[Co(py)_2(H_2PO_2)_2]$: C, 34.60; H, 4.07; N, 8.07. Found: C, 32.82; H, 4.12; N, 7.69.

C. Analytical Data

Analyses of the compounds were made under anhydrous conditions by Galbraith Laboratories, Knoxville, Tennessee.

Melting-point determinations were made on a Mel-Temp melting-point apparatus. The compounds were ground to fine powders in an agate mortar and pestle under nitrogen and placed in the melting-point capillary. No corrections were made on the observed temperatures.

D. Magnetic Susceptibility

Effective magnetic moments of the compounds were obtained using the Gouy method. The equipment consisted of an electromagnet, a power supply, a semimicroanalytical balance, and a sample holder. The electromagnet, power supply, and current regulator were manufactured by Alpha Scientific Laboratories. A Metler analytical balance was used to measure deflections of the sample in the magnetic field. A glass nuclear magnetic resonance tube served as the sample holder and was suspended from the balance pan by a gold chain. The chain and sample tube were protected from air currents by a removable glass tube.

The sample tube was calibrated at a field strength of 5.0 amps using mercury tetrathiocyanatocobaltate(II), which has a magnetic

susceptibility of 16.44 x 10^{-6} per gram.[39] The calibration standard and the complexes were prepared for packing by grinding with an agate mortar and pestle until very powdery. The powder was packed in the sample tube by placing a small amount in the tube and tapping on a wooden surface one hundred times to ensure close packing. This process was repeated for each small addition of sample until the tube was filled to the desired height. All grinding and packing was done in a dry box filled with nitrogen.

The gram magnetic susceptibilities were calculated from the formula:

$$10^6 \chi_g = \frac{\alpha + \beta F'}{w} \qquad (1)$$

where χ_g is the gram magnetic susceptibility, α is a factor to account for the displaced air, β is a calibration factor determined during standardization of the balance, F' is the difference in milligrams between the susceptibility due to the sample tube and the susceptibility of the sample, and w is the weight of the sample in grams. The molar susceptibility, χ_M is obtained by multiplying χ_g by the molecular weight of the sample. The sum of the atomic diamagnetic susceptibilities[40] of the ligands and the metal ion in the complexes was added to χ_M to obtain the corrected χ_M^{corr}. The magnetic moment was then obtained, assuming a Weiss constant of 0°K, from the equation:

$$\mu_{eff} = 2.84\sqrt{\chi_M^{corr} \cdot T} \qquad (2)$$

where μ_{eff} is the effective magnetic moment in Bohr magnetons and T is the absolute temperature. All measurements were made at 23 $\pm$ 2°C.

E. Infrared Spectroscopy

Infrared spectra were obtained for the solid samples as Nujol mulls spread between sodium chloride plates. Perkin-Elmer model 257 and Beckman IR-5A recording spectrophotometers were used to scan the 4000-625 cm^{-1} region. The spectra were calibrated using polystyrene film.

Far-infrared spectra (700-150 cm^{-1} region) were obtained as Nujol mulls sandwiched between polyethylene plates using a Digilab FTS-IR20 spectrometer.

Each mull was prepared by grinding a small amount of the sample with an agate mortar and pestle, adding a few drops of Nujol and then mixing sample and Nujol into a paste. It was necessary to prepare the mulls in a nitrogen atmosphere in the dry box because of the hygroscopic nature of the compounds.

F. Visible and Near-Infrared Spectroscopy

Spectra of the complexes in the visible and near-infrared region were obtained using a Cary 17I recording spectrophotometer manufactured by the Applied Physics Corporation. The spectra of solid samples were obtained as Nujol mulls spread on a piece of Kimwipe. The mull was prepared in a nitrogen atmosphere. Kimwipe saturated with Nujol was placed in the reference beam to equalize light scattering.

Solution spectra of the methanesulfonate complexes were obtained in dichloromethane. The spectra were run in 5- and 10-cm matched quartz cells with solvent in the reference beam.

In obtaining the spectra, the infrared source and detector were used in the 1600-700 nm region and the visible source and detector were used in the 700-300 nm region.

CHAPTER III

RESULTS AND DISCUSSION

A. General Properties

Due to the hygroscopic character of the compounds studied, it was necessary that they be stored in a nitrogen atmosphere.

All $[ML_4(CH_3SO_3)_2]$ complexes (where M = cobalt(II), nickel(II), and copper(II), and L = py and 4-mepy) are soluble in or react with water methanol, dichloromethane, chloroform, nitromethane, and acetonitrile; they are insoluble in benzene, ligroine, and diethyl ether. In <u>para</u>-dioxane, the $[M(py)_4(CH_3SO_3)_2]$ complexes do not dissolve, whereas $[Ni(4\text{-mepy})_4(CH_3SO_3)_2]$ and $[Cu(4\text{-mepy})_4(CH_3SO_3)_2]$ are readily soluble, and $[Co(4\text{-mepy})_4(CH_3SO_3)_2]$ is only slightly soluble. The cobalt(II) and copper(II) complexes are soluble in acetone; nickel(II) complexes are not.

Of the previously mentioned solvents, $[Co(py)_2(CH_3SO_3)_2]$ and $[Ni(py)_2(H_2PO_2)_2]$ are soluble in only water and methanol.

$Co(H_2PO_2)_2$ and $Ni(H_2PO_2)_2$ are soluble only in water.

B. Magnetic Susceptibilities

The results of magnetic susceptibility measurements are summarized in Table III. The values for the cobalt(II) and nickel(II) compounds are typical of high-spin octahedral stereochemistries. Because the magnetic moments for monomeric (magnetically dilute) copper(II) complexes occur in the range of 1.8-2.0 BM regardless of stereochemistry about the copper atom, these data do not provide a

TABLE III

MAGNETIC SUSCEPTIBILITIES

Compound	$X_M \times 10^6$	Molar Diamagnetic Correction $\times 10^6$	$X_M^{corr} \times 10^6$	μ_{eff} BM
$Co(H_2PO_2)_2$	10,523	74	10,597	5.03
$[Co(py)_2(CH_3SO_3)_2]$[a]	---	--	---	---
$[Co(py)_4(CH_3SO_3)_2]$	11,535	56	11,591	5.26
$[Co(4\text{-mepy})_4(CH_3SO_3)_2]$	11,196	104	11,300	5.20
$Ni(H_2PO_2)_2$	4620	74	4694	3.36
$[Ni(py)_2(H_2PO_2)_2]$	3878	63	3941	3.07
$[Ni(py)_4(CH_3SO_3)_2]$	4123	56	4179	3.17
$[Ni(4\text{-mepy})_4(CH_3SO_3)_2]$	4201	104	4305	3.20
$[Cu(py)_4(CH_3SO_3)_2]$	1277	56	1333	1.78
$[Cu(4\text{-mepy})_4(CH_3SO_3)_2]$	1371	104	1475	1.88

[a]Not enough sample was obtained to make this measurement.

means to determine whether or not the methanesulfonate anion is coordinated.

C. Infrared Spectra

1. Methanesulfonate Bands

The methanesulfonate anion has a tetrahedral structure and belongs to the C_{3v} point group. If the anion is represented as XSO_3^- (where X = CH_3), there should be six normal modes of vibration,[10] all of which would be active in both the Raman and infrared spectrum. The three totally symmetric (A_1) vibrations include an SO_3 symmetric bend. The asymmetric (E) vibrations can be described as an SO_3 asymmetric stretch, an SX wag, and an SO_3 asymmetric bend.[10]

On coordination through an oxygen atom (as in X-SO_2-O*, where X represents CH_3 and O* represents the coordinating oxygen atom), the symmetry is lowered to C_s. No degeneracy exists in this point group and nine fundamental vibrations are expected. These vibrations[10] may be described as SO_2 symmetric and asymmetric stretches, an SO_2 bending mode, SX and SO* stretches, an SO_2 rock, an SX wag, an SO* wag and a torsion. All vibrations for C_s symmetry are infrared and Raman active.

Vibrational assignments for the anion and for coordinated methanesulfonate are presented in Table IV. The methanesulfonate bands for the complexes studied are tabulated in Table V. Figures 1 and 2 present the infrared spectra of $[Co(py)_4(CH_3SO_3)_2]$ and $[Cu(4\text{-mepy/py})_4\text{-}CH_3SO_3)_2]$, respectively, in the 1700-700 cm^{-1} region. Absorption bands at 1470 and 1380 cm^{-1} are due to Nujol.

Assignments made in this work are based upon comparison of the vibrational frequencies of ionic KCH_3SO_3 with those of the coordinated

TABLE IV

INFRARED ABSORPTIONS (cm^{-1}) OF IONIC AND COORDINATED CH_3SO_3 GROUPS

C_{3v} Symmetry		C_s Symmetry		
$CH_3SO_3^{-a}$	Assignment	$CH_3SO_3H^b$	$CH_3SO_2OCH_3^c$	Assignment
1183	SO_3 asymmetric stretching (E)	1350	1370	SO_2 asymmetric stretching (A")
1049	SO_3 symmetric stretching (A_1)	1174	1176	SO_2 symmetric stretching (A')
		904	1010	S-O* stretching (A')
785	S-CH_3 stretching (A_1)	772	727	S-CH_3 stretching (A')
554	SO_3 symmetric bend (A_1)	535	555	SO_2 bend (A')
523	SO_3 asymmetric bend (E)	506	530	SO_2 rock (A")
		480		S-O* wag (A')
		420		torsion (A")
346	S-CH_3 wag (E)	338		S-CH_3 wag (A')

TABLE IV (Continued)

[a]Source: R. J. Gillespie and E. A. Robinson, Can. J. Chem., 40, 644 (1962).

[b]Source: H. Gerding and J. W. Maarsen, Rec. Trav. Chim. Pays-Bas, 77, 374 (1958).

[c]Source: A. Simon, H. Kriegsmann, and H. Dutz, Chem. Ber., 89, 2378 (1956).

TABLE V

CH_3SO_3 VIBRATIONAL FREQUENCIES (cm^{-1}) IN COMPLEXES

$[M(py)_4(CH_3SO_3)_2]$ Co	Ni	Cu	$[M(4\text{-mepy})_4(CH_3SO_3)_2]$ Co	Ni		$[Co(py)_2(CH_3SO_3)_2]$	Assignment
1255	1248	1235	1252	1249	1245	1258 broad 1200	SO_2 asymmetric stretching
1172	1170	1183 1144	1170	1170	1187	1170 broad	SO_2 symmetric stretching
1051	1051	1045	1050	1043	1048	1045 broad	S-O* stretching
774	770	772	780	770	770	770 725	S-CH_3 stretching
550	550	552	550	552	551		SO_2 bend
532	531	527	535	534	525	575-510 broad	SO_2 rock
516	516		517	517			S-O* wag
364	360		350	360		350 broad	torsion
340	340	343	341	340	340		S-CH_3 wag

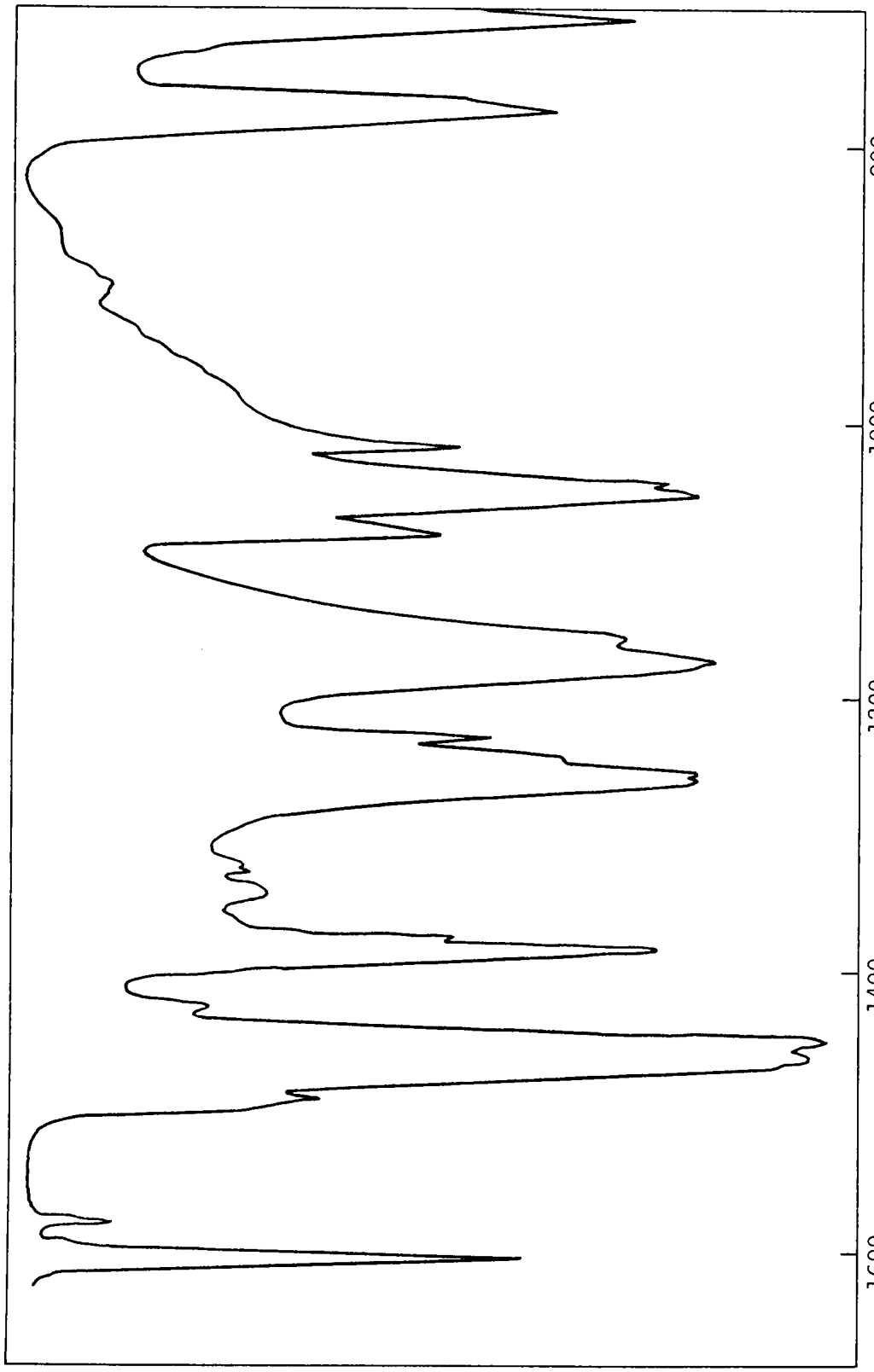

Figure 1. Infrared spectrum of $[Co(py)_4(CH_3SO_3)_2]$.

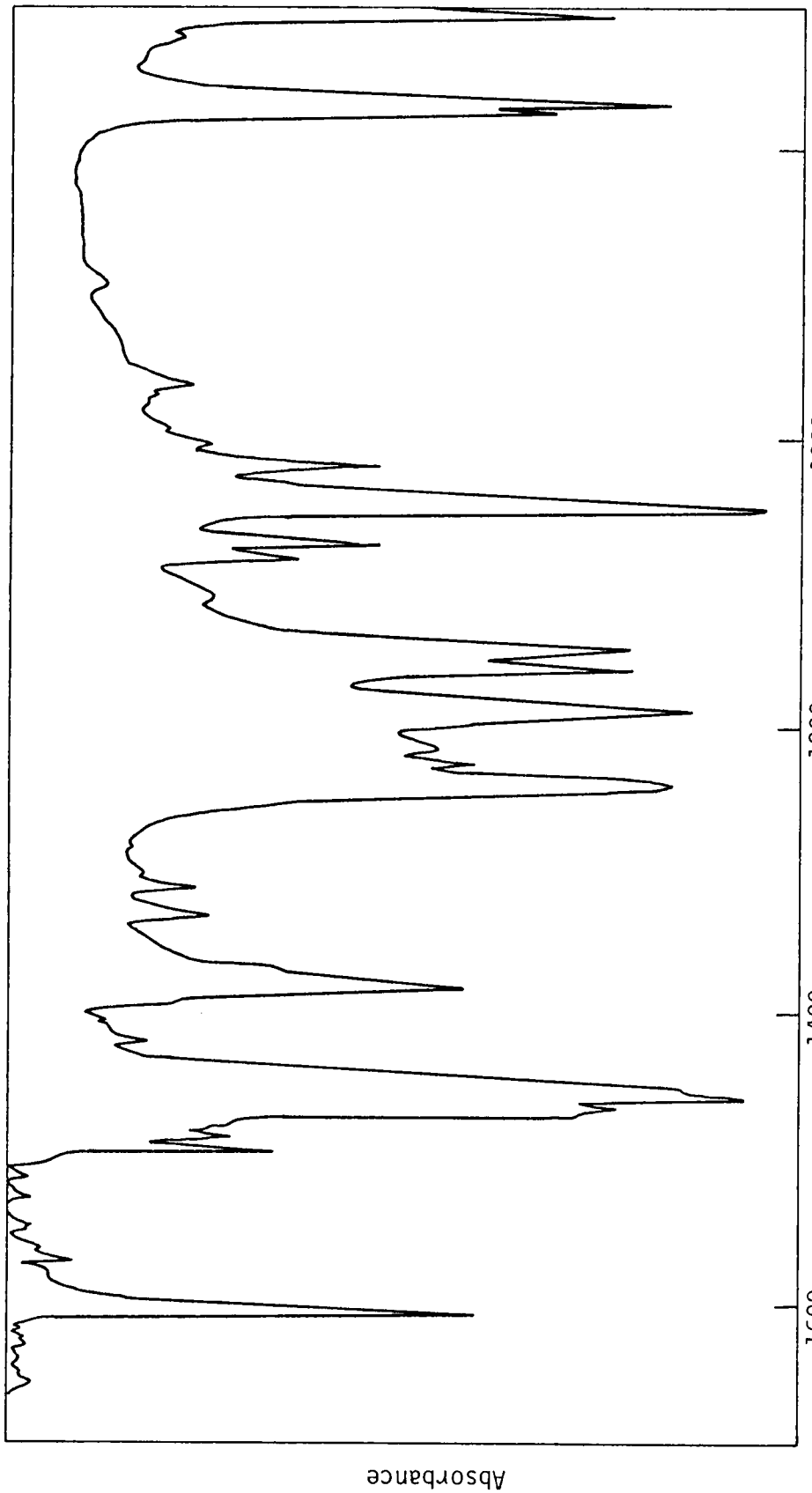

Figure 2. Infrared spectrum of $[Cu(4\text{-mepy})_4(CH_3SO_3)_2]$.

CH_3SO_3 group. The SO_3 symmetric stretch at 1049 cm^{-1} is observed to shift to higher frequency (by approximately 120 cm^{-1}) upon coordination as would be expected due to the increased double bond character of the SO bonds. The SO_3 asymmetric stretch at 1183 for the anion splits on complexation to give a new band at 1250 cm^{-1} and another band at 1050 cm^{-1}; a greater splitting is observed for the parent acid. This band splitting is consistent with the fact that upon coordination the degeneracy of the asymmetric stretching mode is lifted. Similar splitting effects are observed on coordination for the degenerate SO_3 asymmetric bend and the degenerate SX wag (523 and 346 cm^{-1}, respectively) in the anion.

Based upon infrared spectral information, it is concluded that only one type of CH_3SO_3 group is present and that the spectral data is consistent with monodentate coordination in the tetrapyridine and tetrakis(4-methylpyridine) cobalt(II) and nickel(II) compounds.

In both copper complexes, the methanesulfonate group is considered to be only weakly coordinated or "semi-coordinated." The degeneracy of the SO_3 asymmetric stretch vibration is lifted to give new bands around 1240 and 1045 cm^{-1} as would be expected on coordination. However, neither of the degenerate modes for the anion in the far-infrared is split.

The infrared spectrum of $[Co(py)_2(CH_3SO_3)_2]$ in the 1400-900 cm^{-1} region consists of very broad bands which could not be completely resolved. The absorptions are listed in Table V, p 21; it appears as though more than one type of CH_3SO_3 group is present. The overlapping of absorptions associated with two different environments for the

methanesulfonate group could give rise to the observed spectrum. One CH_3SO_3 group might be bidentate with the second ionic. Another possibility which is preferred by the author is that one CH_3SO_3 is bridging between cobalt centers while the second CH_3SO_3 is associated with only one cobalt. This latter suggestion is consistent with the low solubility of the compound in non-coordinating solvents.

2. Hypophosphite Bands

The two hydrogen and two oxygen atoms in the hypophosphite anion have a tetrahedral disposition about the phosphorus and thus the ion belongs to the C_{2v} point group. According to group theoretical methods, $H_2PO_2^-$ should have nine fundamental vibrations, eight of which would be infrared active.[29] The four totally symmetric (A_1) vibrations can be described as a PH_2 symmetric stretch, a PH_2 scissor, a PO_2 symmetric stretch, and a PO_2 scissor. The asymmetric vibrations include PH_2 and PO_2 asymmetric stretches, a PH_2 wag, and a PH_2 rock. The PH_2 twisting motion is infrared inactive. Vibrational assignments are given in Table VI.

The frequency relation of the PH_2 symmetric and asymmetric vibrations[22,26] is the reverse of that found for CH_2, NH_2, and OH_2 where the asymmetric vibration occurs at the higher frequency. The relative intensities of the PH_2 stretching bands in the Raman and infrared spectra and their depolarization ratios in the Raman spectrum suggest that the high frequency band arises from the PH_2 symmetric stretch and the low frequency band from the asymmetric vibration.

Hypophosphorous acid has C_1 symmetry[26] and all twelve fundamental modes of vibration are infrared and Raman active. The same PH_2

TABLE VI

INFRARED ABSORPTIONS (cm^{-1}) OF IONIC AND COORDINATED H_2PO_2 GROUPS[a]

C_{2v} Symmetry			C_1 Symmetry		
$H_2PO_2^-$[b] (-190°C)	$H_2PO_2^-$[c] Room Temperature	Assignment	H_3PO_2[b] (-180°C)	$Ca(H_2PO_2)_2$[b] Room Temperature	Assignment
2361	2375m	PH_2 symmetric stretching (A_1)	2388		PH_2 symmetric stretching
2318	2312s	PH_2 asymmetric stretching (B_1)	2319	2383	PH_2 asymmetric stretching
1187	1230s	PO_2 asymmetric stretching (B_2)	1184	1184	P=O stretch
1167	1171s	PH_2 scissor (A_1)	1124	1147	PH_2 scissor
1090	1080w	PH_2 wag (B_2)	1055	1098	PH_2 wag
1073	1046s	PO_2 symmetric stretching (A_1)	950	1063	P-O* stretch
				926	PH_2 twist
812	808s	PH_2 rock (B_1)	803	809	PH_2 rock
472	476s	PO_2 scissor (A_1)	428	460	O*-P=O scissor

TABLE VI (Continued)

[a]s, Strong; m, medium; w, weak.

[b]Source: R. W. Lovejoy and E. L. Wagner, J. Phys. Chem., 68, 544 (1964).

[c]Source: M. Tsuboi, J. Am. Chem. Soc., 79, 1351 (1957).

vibrations (plus the PH_2 twist) are expected for the acid as for the anion. The PH_2 twist should give rise to a band near 900 cm^{-1} but it was not detected. The frequencies of the PH_2 scissor and PH_2 wag vibrations were lowered nearly forty wavenumbers. The phosphorus-oxygen modes are somewhat different from those of the salts and consist of a P=O stretch, a P-O* stretch, and a 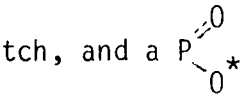 scissor deformation. The vibrational assignments for the acid and for the calcium salt which also has C_1 symmetry[26] are presented in Table VI (p 26).

If bidentate coordination of the hypophosphite group occurred as either a chelating or bridging ligand, it would possess local C_{2v} symmetry. Eight infrared active vibrations would be expected and the P-O bond order would approximate a value of one. Similar to the F_2PO_2 group,[41] the PH stretching modes should be found at higher frequency for bidentate hypophosphite coordination than for monodentate groups. The asymmetric PO stretching mode would be lowered considerably whereas the symmetric mode would shift little. The net result would be a lowering of the average PO stretch. This lowering is caused to some extent by charge withdrawal from the phosphorus-oxygen into the metal-oxygen bond region. Back donation from the oxygen lone pairs to phosphorus can partially compensate for the charge withdrawal and can account for the observed increase in the PH stretching frequencies.[41]

All hydrated hypophosphite salts absorb in the 3300 and 1640 cm^{-1} regions,[32] which presumably correspond to O-H stretching and bending, respectively. Frequencies higher than 3450 cm^{-1} are absent in most salts indicating that no completely free O-H stretching occurs and that hydrogen bonding is probable. Most salts give several sharp peaks

between 3450 and 2860 cm^{-1} due to more than one type of hydrogen bonding.

Comparison of anhydrous and hydrated hypophosphite salts[32] reveals several differences in the spectra below 1500 cm^{-1}. When hydrated, a general shift of peaks to lower frequencies occurs; the PO stretching region is especially sensitive to hydration. The frequency of the PH_2 rock has been observed to split into a doublet or triplet in the anhydrous salt.[32]

The vibrations for the hypophosphite group in the nearly anhydrous cobalt(II) and nickel(II) hypophosphites and estimated intensities are listed in Table VII. Figures 3 and 4 present the spectra of these compounds in the 2500-2200 cm^{-1} and the 1250-800 cm^{-1} regions.

Neither compound absorbs above 2550 cm^{-1}. Nickel hypophosphite weakly absorbs at 1650 cm^{-1} possibly due to O-H bending; there is no corresponding absorption for the cobalt compound. The PH_2 symmetric and asymmetric stretching vibrations are shifted to higher frequencies as would be expected on coordination. The large number of bands in the 1200 to 1000 cm^{-1} region suggests that more than one type of H_2PO_2 group is present. Since the anion vibrations are nondegenerate, the bands cannot be the result of symmetry reduction by covalent bond formation.

The PH_2 rock (at 808 cm^{-1} in the anion) splits into two components in the $Co(H_2PO_2)_2$ spectrum. Since this vibration is not degenerate, the splitting presumably indicates that more than one type of H_2PO_2 group is present. A band considerably wider than a normal single absorption is

TABLE VII

HYPOPHOSPHITE VIBRATIONS IN ANHYDROUS COMPOUNDS (cm^{-1})[a]

$Co(H_2PO_2)_2$	$Ni(H_2PO_2)_2$	$[Ni(py)_2(H_2PO_2)_2]$
2430s	2420sh	---
2370s	2390-2340s	2380-2275[b]m
1160s	1190-1140s	1175-1165s
1145sh		
1120s		1130sh
1085s	1080s	1090m
1070m	1060sh	1062m
1055s	1045-1015s	1030-1015m
1005w		
825s	820[b]s	808[b]s
805s		
510s	500s	513s

[a]s, Strong; m, medium; w, weak; sh, shoulder.

[b]Band broader than a single absorption but could not be resolved.

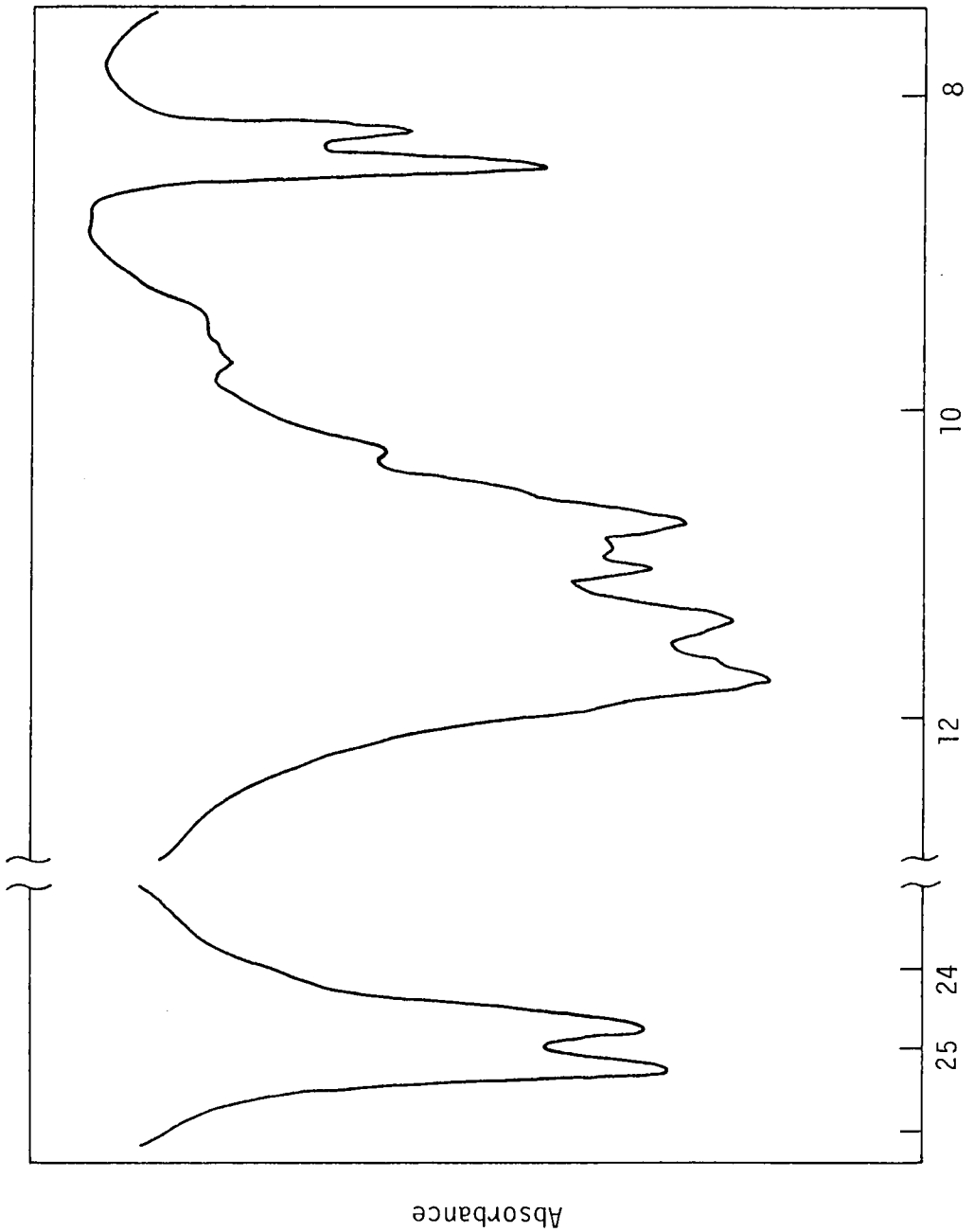

Figure 3. Infrared spectrum of $Co(H_2PO_2)_2$.

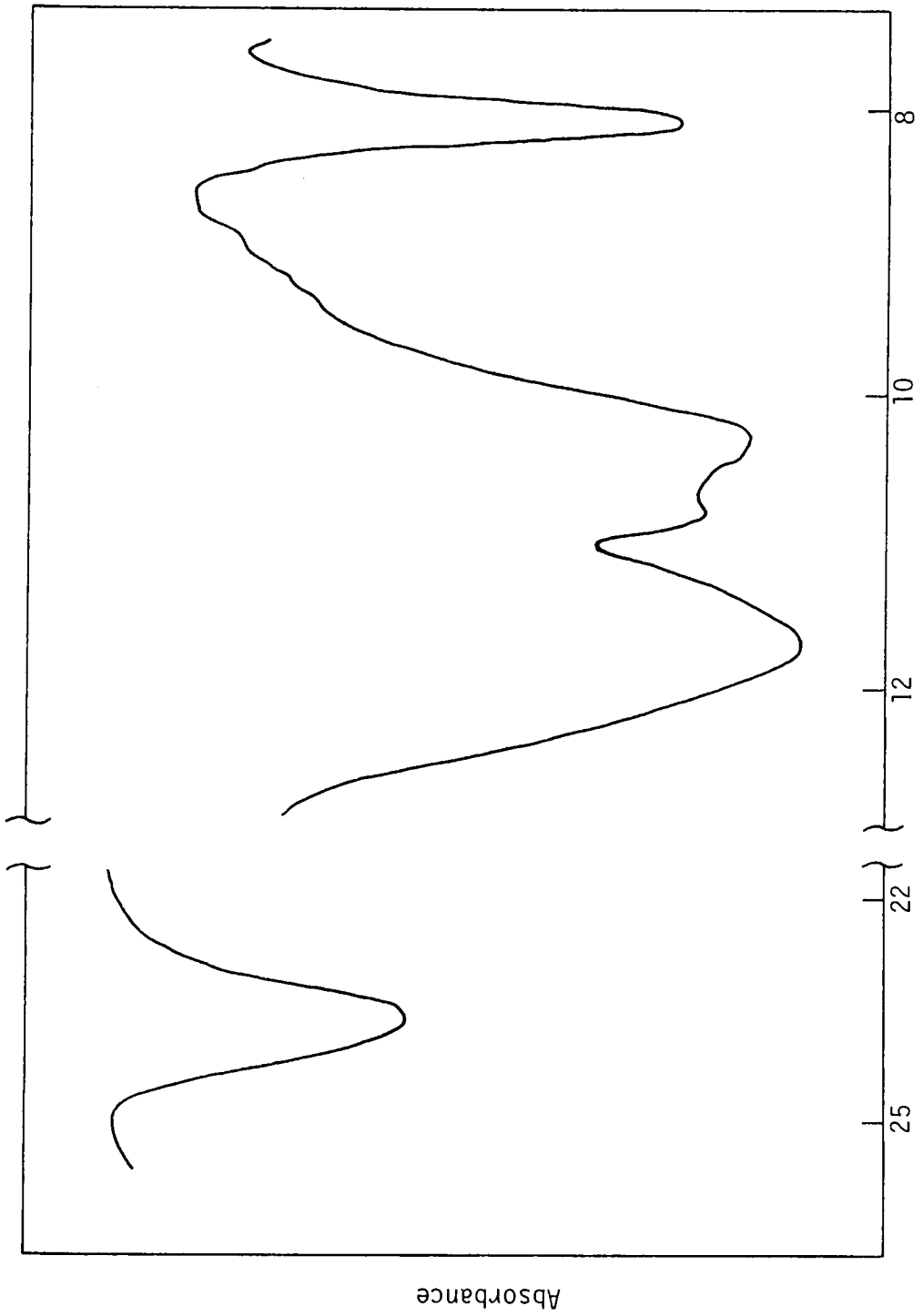

Figure 4. Infrared spectrum of $Ni(H_2PO_2)_2$.

observed in this region for the nickel(II) compound; it is expected that two absorptions are present but were not resolved.

The PO_2 scissor motion in the anion occurs at 476 cm^{-1}. Because this vibration has been shifted approximately 30 cm^{-1} to higher frequency in $Co(H_2PO_2)_2$ and in $Ni(H_2PO_2)_2$, coordination to the metal atom is indicated.

The observed frequencies in the 1200 to 1000 cm^{-1} region indicate that more than one type of hypophosphite group is present in these compounds. Infrared and far-infrared spectra have established coordination to the metal atom. If monodentate groups are present, certain spectral features should be found: (1) a P-O stretch at higher frequency than the asymmetric PO_2 stretch in the anion, (2) a P-O* (O* representing oxygen covalently bound to the metal) stretch at lower frequency than the PO_2 symmetric stretch of the ion because of reduced PO bond order, and (3) a significantly greater difference between the PO stretching vibrations than for the anion. Those features were not observed in the spectra of $Co(H_2PO_2)_2$ and $Ni(H_2PO_2)_2$. In conjunction with electronic spectral data and magnetic susceptibility values which indicate hexacoordination about the metal, it seems reasonable to postulate the presence of both chelating and bridging bidentate hypophosphite ligands. A clear distinction between bidentate bridging and chelating ligands cannot be made with vibrational spectra; therefore, definite assignments for PO stretching vibrations in $Co(H_2PO_2)_2$ and in $Ni(H_2PO_2)_2$ are not possible.

The hypophosphite vibrations for $[Ni(py)_2(H_2PO_2)_2]$ are listed in Table VII. It is difficult to ascertain the extent of coordination

of the hypophosphite group to the metal atom in this compound. A single broad absorption centered at 2300 cm^{-1} is detected in the PH stretching region. In conjunction with hexacoordination about the metal atom, the position and number of vibrations between 1200 to 1000 cm^{-1} suggest the presence of two types of bidentate hypophosphite groups. The PH_2 rock was not split; however, the band is too broad for a single absorption. The PO_2 scissoring motion is found at considerably higher frequency than in the anion, presumably due to coordination to the metal atom.

It is unlikely that intermolecular hydrogen bonding is an explanation for the broad bands in $Ni(H_2PO_2)_2$ and in $[Ni(py)_2(H_2PO_2)_2]$. David and Hallam[42] studied the hydrogen bonding ability of the PH group in a series of phosphonate esters. The PH group was found to be barely capable of forming hydrogen bonds even with the most powerful proton-accepting solvents. Intermolecular association was absent in the pure compounds.

3. Pyridine Bands

Gill and coworkers[43] have found a direct correspondence between complexed and free pyridine vibrational frequencies. Such behavior should be expected because to a first approximation the vibrations of pyridine coordinated to a heavy metal atom do not involve the metal-nitrogen bond. For this study, the coordinated pyridine and 4-methylpyridine vibrations were ascertained by direct comparison with the uncomplexed bases. The pyridine bands at 1578, 601, and 403 cm^{-1} are especially sensitive to coordination and are shifted 30 $\pm$ 5 cm^{-1} to

higher frequency upon coordination. Similar behavior is noted for the 1605, 513, and 483 cm^{-1} bands of 4-methylpyridine. The bands observed for free and coordinated pyridine and 4-methylpyridine in the 1650-200 cm^{-1} region are listed in Table VIII.

Splitting of the bands occurs in several of the spectra and is probably caused by coupling effects between pyridine or 4-methylpyridine molecules within the unit cell and by symmetry distortions within the crystalline lattice.

4. Metal-Ligand Bands

One infrared active metal-nitrogen vibration is expected for these octahedral or tetragonal (D_{4h} symmetry) compounds.[44] For monomeric octahedral complexes, the metal-pyridine nitrogen asymmetric stretch has been found to occur in the 200-287 cm^{-1} range.[44] The metal-(4-methylpyridine) nitrogen vibration should be found at lower frequency because of the increased effective mass of the ring.

The metal-nitrogen vibration is split in some of the complexes, presumably due to solid state effects or distortion from octahedral symmetry. The metal-nitrogen vibrations are listed in Table IX. The infrared spectra of these complexes indicate that all pyridine and 4-methylpyridine molecules are coordinated to metal ions.

One metal-oxygen vibration is expected for these compounds containing coordinated anions.[44] The metal-oxygen vibrational frequencies of the bismethanesulfonatotetrapyridine complexes follow the trend found in their metal-nitrogen vibrations: Cu > Ni > Co. That a metal-oxygen frequency was observed for only bismethanesulfonatotetrakis(4-methylpyridine)copper(II) suggests that the metal-oxygen

TABLE VIII

INFRARED ABSORPTIONS OF FREE AND COORDINATED PYRIDINE AND 4-METHYLPYRIDINE

Compound	Vibrational Frequencies (cm^{-1})[a,b]					
Pyridine	1601s	1578s	1488s	1443s	1220m	1150m
	1070m	1032s	993s	745s	699s	650[c]
	601[c]	403[c]				
$[Co(py)_2(CH_3SO_3)_2]$	1602s	1576m	1490sh	1455s	1200m	1160m
	1015w	708s	633	433		
$[Co(py)_4(CH_3SO_3)_2]$	1609s	1578w	1491m	1453s	1228m	1157s
	1075m	1045sh	1015m	765sh	703s	630
	427					
$[Ni(py)_4(CH_3SO_3)_2]$	1603s	1585w	1488w	1450s	1224s	1152s
	1072m	1041s	1011m	763s	706s	632
	432					
$[Cu(py)_4(CH_3SO_3)_2]$	1608s	1498m	1452s	1222m	1152s	1144m
	1080w	1072m	1045s	1017m	768s	772m
	705s	701s	642	435	424	
$[Ni(py)_2(H_2PO_2)_2]$	1601m	1490sh	1453s	1222m	1149s	1078m
	1040s	990w	763s	709s	632	440
4-Methylpyridine	1605s	1568m	1500m	1447m	1416s	1384w
	1225m	1214w	1069w	1040w	997s	970w
	800s	730m	513[d]	483[d]		
$[Co(4\text{-mepy})_4(CH_3SO_3)_2]$	1628s	1570w	1519m	1510m	1460s	1435m
	1337m	1235m	1215m	1075m	1020s	820s
	735m	541	495			
$[Ni(4\text{-mepy})_4(CH_3SO_3)_2]$	1625s	1568w	1515w	1458s	1327w	1213w
	1052sh	1020m	828m	815m	739m	547
	500					
$[Cu(4\text{-mepy})_4(CH_3SO_3)_2]$	1620s	1510w	1237m	1217m	1075w	1035m
	835sh	825m	820m	731m	550	498

[a] s, Strong; m, medium; w, weak; sh, shoulder.

[b] Bands due to the complexed pyridine bases in the regions near 1450 and 1380 cm^{-1} were obscured by Nujol absorption.

TABLE VIII (Continued)

[c]Source: N. S. Gill, R. H. Nuttall, D. E. Scalfe, and D. W. A. Sharp, J. Inorg. Nucl. Chem., 18, 79 (1961).

[d]Source: D. H. Brown, R. H. Nuttall, J. McAvoy, and D. W. A. Sharp, J. Chem. Soc., 892 (1966).

TABLE IX

INFRARED ABSORPTIONS OF METAL-LIGAND VIBRATIONS
(cm^{-1})

Compound	M-N	M-O
$[Co(py)_4(CH_3SO_3)_2]$	233	170
$[Ni(py)_4(CH_3SO_3)_2]$	248	180
$[Cu(py)_4(CH_3SO_3)_2]$	268	237
$[Co(4\text{-mepy})_4(CH_3SO_3)_2]$	210 260	
$[Ni(4\text{-mepy})_4(CH_3SO_3)_2]$	225 265	
$[Cu(4\text{-mepy})_4(CH_3SO_3)_2]$	240 285	215
$[Co(py)_2(CH_3SO_3)_2]$	225, broad	180
$[Ni(py)_2(H_2PO_2)_2]$	195 245	265
$Co(H_2PO_2)_2$		280
$Ni(H_2PO_2)_2$		320

vibrations for the corresponding cobalt(II) and nickel(II) complexes occur below 170 cm^{-1} and supports the trend found in the tetrapyridine complexes.

The metal-oxygen vibration for the anhydrous hypophosphites is found around 300 cm^{-1}. This vibration in $[Ni(py)_2(H_2PO_2)_2]$ was assigned as that band at 265 cm^{-1}.

Metal-oxygen frequencies for these compounds are listed in Table IX (p 38).

D. Visible and Near-Infrared Spectra

1. Introduction

The five 3d orbitals of first-row transition metal ions are degenerate in the free ion. In the presence of a cubic field these orbitals are split into a triply degenerate and doubly degenerate set of orbitals. In an octahedral field the orbitals of lower energy are those of the triply degenerate set (t_{2g}); the doubly degenerate set (e_g) is of higher energy.[45] The relationship between the free ion orbitals and the orbitals in an octahedral field is shown in Figure 5. Tetragonal distortion of the octahedral arrangement can be caused by a decrease in ligand field strength along the z-axis. An extreme distortion of this type will result in a square-planar configuration.

The crystal field model gives a qualitative description of the splitting of the degenerate d orbitals but actual energy separations can be obtained only through detailed calculation from spectral data. This model also treats ligands as point charges or dipoles and does not consider covalent interaction between the metal ion and the ligand

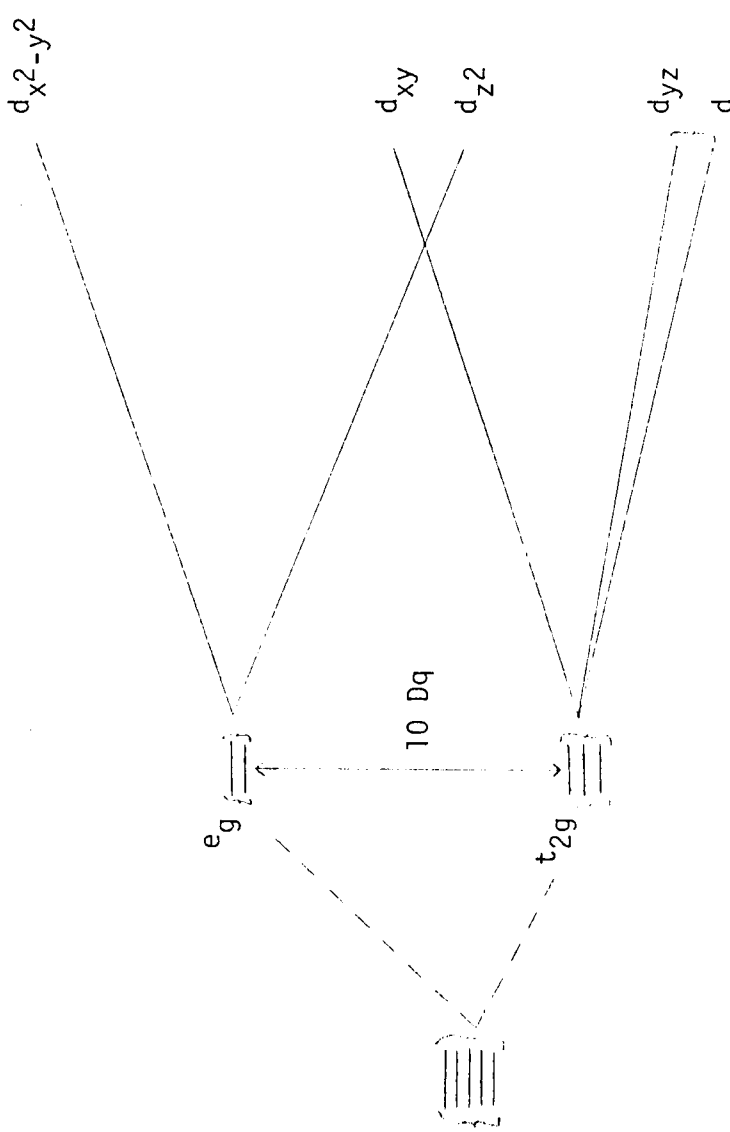

Figure 5. Splitting of 3d orbitals in octahedral and tetragonally distorted octahedral fields.

atoms. Whenever possible, parameters taking into account the degree of covalency will be employed.

2. Cobalt(II) Spectra

The cobalt(II) ion has a d^7 electron configuration which gives rise to the ^4F free-ion spectroscopic ground state. An octahedral crystal field removes the orbital degeneracy to make $^4T_{1g}(F)$ the ground state in a weak-field electronic configuration. Three spin-allowed transitions are predicted for the cobalt(II) ion in an octahedral field;[46] they are presented in Figure 6. The $^4T_{1g} \rightarrow {}^4T_{2g}$ transition (ν_1) occurs in the 10,000 to 8,000 cm^{-1} region and is not as intense as the highest energy visible band (ν_3), $^4T_{1g} \rightarrow {}^4T_{1g}(P)$. The latter transition often shows multiple structure which may be the result of spin-orbit coupling, low symmetry, and/or spin-forbidden transitions.[47] The weak theoretically forbidden two-electron transition (ν_2), $^4T_{1g} \rightarrow {}^4A_{2g}$, normally occurs at energies intermediate to those of ν_1 and ν_3 and is usually obscured by the latter transition.[48]

In a tetragonally distorted octahedral field (D_{4h} symmetry) produced by a decrease in ligand field strength along the z-axis, the ^4T terms are split due to symmetry lowering. The ν_1 and ν_3 absorption bands observed in octahedral symmetry should each consist of two components in D_{4h} symmetry, while the ν_2 band should still correspond to a single transition.[49] If the tetragonal distortion is small, broadening of the ν_1 and ν_3 absorption bands will be observed, but as the distortion is increased, the ν_1 and ν_3 bands should be resolved into their components. The electronic spectrum can be further complicated by spin-orbit coupling, low symmetry, and spin-forbidden transitions.

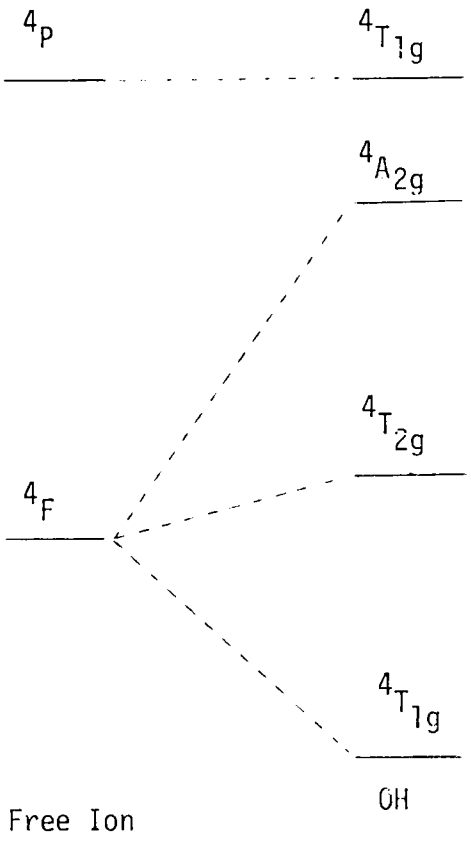

Figure 6. Splitting of the ^4P and ^4F states of cobalt(II) in an octahedral crystal field.

a. Methanesulfonate compounds. The mull spectra of $[Co(py)_4(CH_3SO_3)_2]$ and $[Co(4\text{-mepy})_4(CH_3SO_3)_2]$ reveal a broad near-infrared band around 8000 cm^{-1} and a visible band near 20,000 cm^{-1} containing multiple structure. The spectra are presented in Figures 7 and 8, respectively and the main features observed in the mull spectra are listed in Table X. The spectral band positions and intensities are characteristic of octahedral complexes with moderate tetragonal distortion.

Ballhausen and Jorgensen state[46] that cis- and trans- complexes $[CoL_4X_2]$ are expected to exhibit two bands in the visible region. They further explain that cis- complexes have only broad bands in contrast to the trans- complexes where there is a distinct separation into two bands since the splitting in trans- complexes is generally twice that of the corresponding shift in cis- complexes. Therefore, since at least two peaks are seen in the visible band, it is believed that $[Co(py)_4(CH_3SO_3)_2]$ and $[Co(4\text{-mepy})_4(CH_3SO_3)_2]$ have CH_3SO_3 groups in trans- positions.

From the close agreement of absorption bands for mull and dichloromethane solution spectra of $[Co(py)_4(CH_3SO_3)_2]$ and $[Co(4\text{-mepy})_4(CH_3SO_3)_2]$, it seems that no significant decomposition has occurred on dissolution in dichloromethane.

A Nujol mull spectrum of $[Co(py)_2(CH_3SO_3)_2]$ in the visible and near-infrared region is given in Figure 9, and absorption maxima are tabulated in Table X. From the broad nearly symmetrical bands at 7940 and 20,000-18,000 cm^{-1}, it is inferred that tetragonal distortion is small.

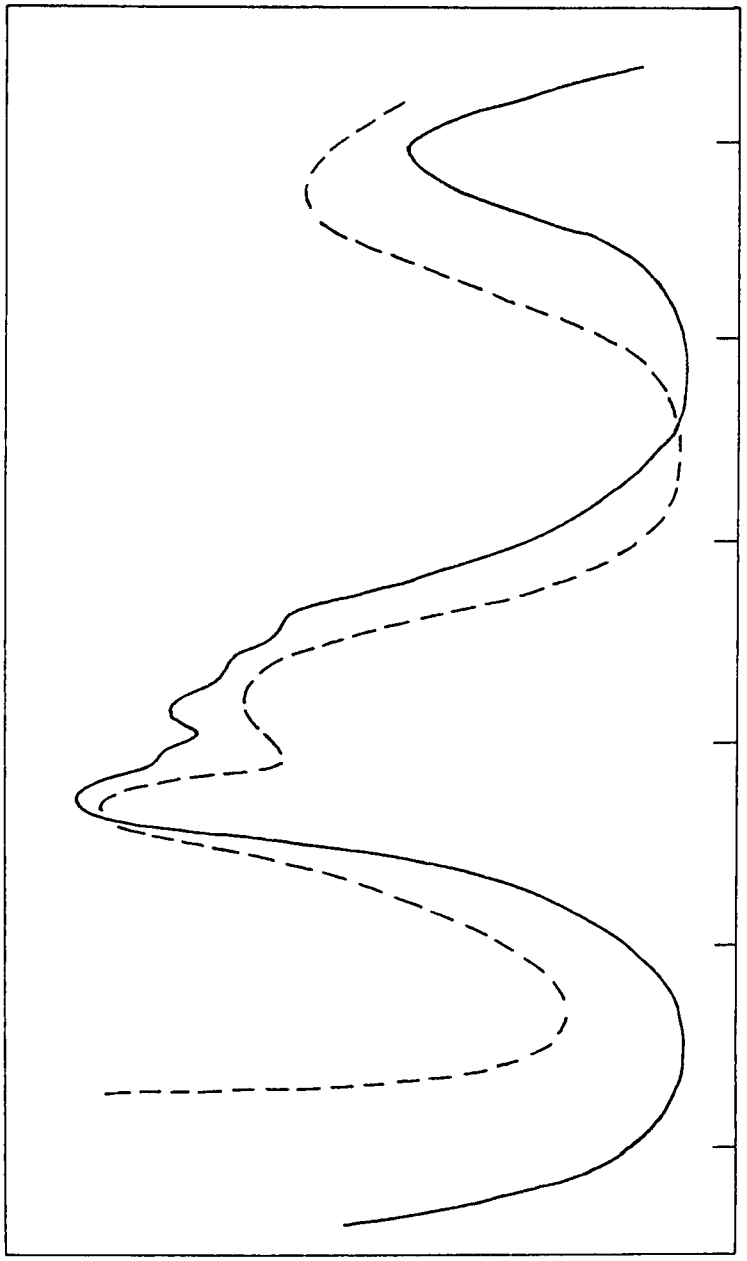

Figure 7. Visible and near-infrared spectra of $[Co(py)_4(CH_3SO_3)_2]$ as a Nujol mull (dotted line) and as a dichloromethane solution (solid line).

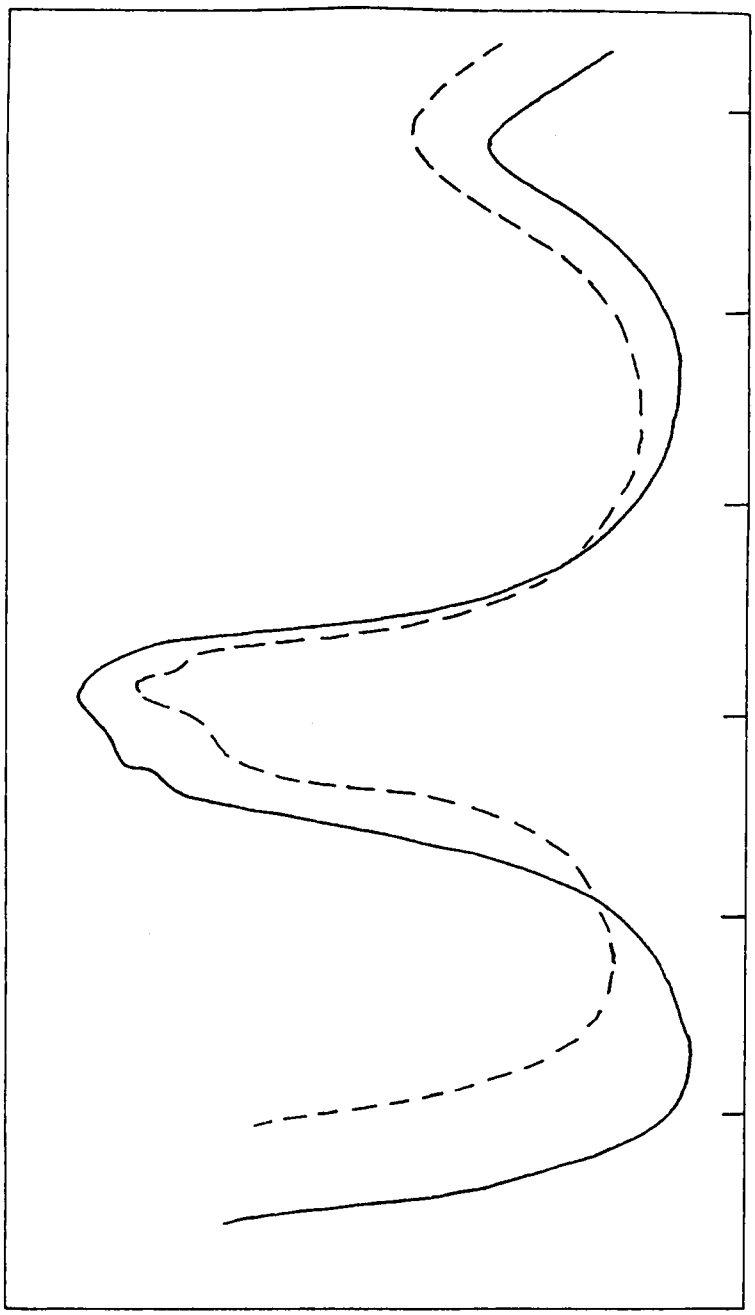

Figure 8. Visible and near-infrared spectra of $[Co(4\text{-mepy})_4(CH_3SO_3)_2]$ as a Nujol mull (dotted line) and as a dichloromethane solution (solid line).

TABLE X

ELECTRONIC SPECTRAL DATA FOR COBALT(II) COMPOUNDS

Compound	Absorption Maxima (cm^{-1})[a]					10Dq	B'	β
	ν_1			ν_3				
$[Co(py)_4(CH_3SO_3)_2]$	9000m		19,200s	21,100vs		10,200	887	0.91
$[Co(4\text{-mepy})_4(CH_3SO_3)_2]$	8330m		19,000sh	19,400vs	20,600sh	9430	811	0.84
$[Co(py)_2(CH_3SO_3)_2]$	7940m	14,900m		18,900vs		9000	801	0.82
$[Co(H_2PO_2)_2$	7870m	17,200s	19,500sh	20,200vs	21,100sh	9020	893	0.92

[a] vs, Very strong; s, strong; m, medium; sh, shoulder.

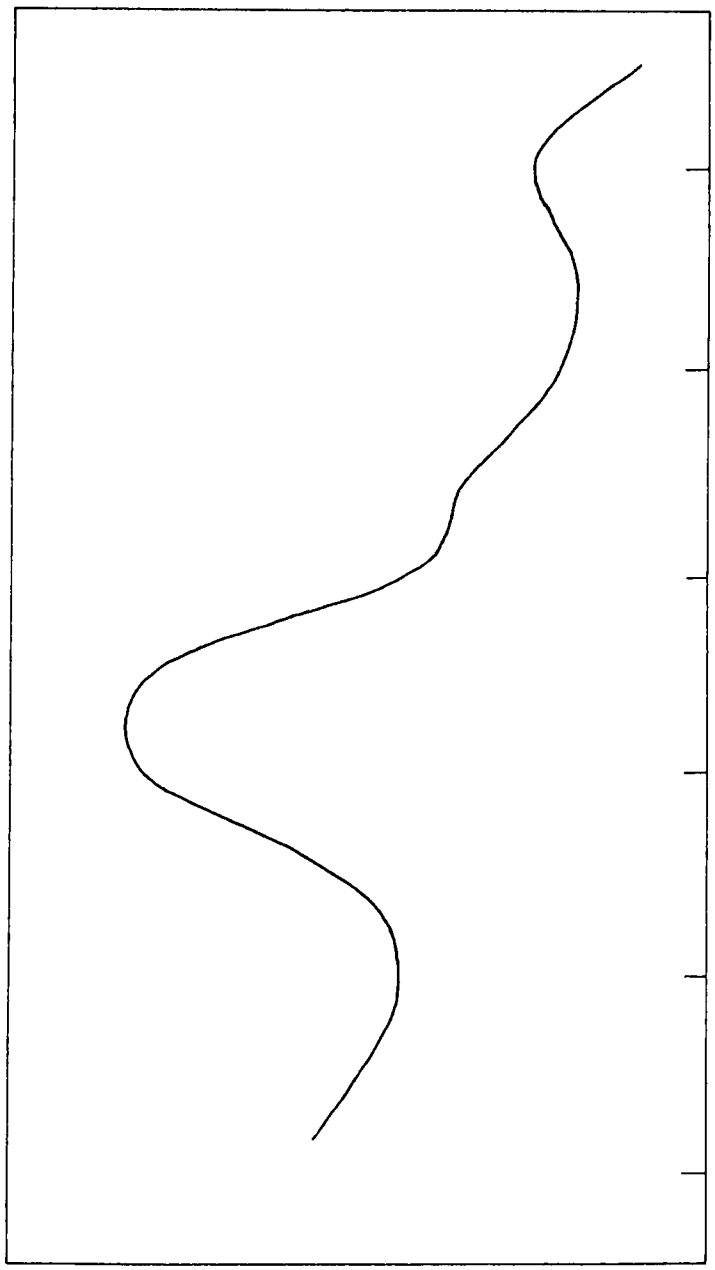

Figure 9. Visible and near-infrared spectrum of $[Co(py)_2(CH_3SO_3)_2]$ as a Nujol mull.

D_q values have been calculated for these approximately octahedral species using the energy matrix for the two $^4T_{1g}$ levels which is given by[50]

$$\begin{vmatrix} -6\,D_q - E & 4\,D_q \\ 4\,D_q & X - E \end{vmatrix} = 0 \qquad (3)$$

where the energies from the center of gravity of the ^4F state are $2D_q$ and $12D_q$ for the $^4T_{2g}$ and $^4A_{2g}$ states, respectively. The symbol x refers to the energy difference between the centers of gravity of the ^4F and ^4P states. The value of $x_{\text{free Co(II)}}$ is equal to 15B and x_{complex} equals 15B'. B' is then found after the energy matrix has been solved for x. The value of the Racah parameter B (where B' corresponds to the complexed ion and B to the free ion) is a measure of the energy separation between Russell-Saunders states of the same multiplicity.[51] The amount of lowering of B' from the free ion B value is an indication of the extent of covalency in the complex; a large decrease in the B value indicates considerable covalency. The nephelauxetic ratio β (B'/B) is another means of measuring the covalency of metal-ligand interaction.[51] D_q, B', and β values have been listed for the methanesulfonate complexes in Table X (p 46).

b. Hypophosphite compound. Figure 10 presents the Nujol mull spectrum of $Co(H_2PO_2)_2$ in the visible and near-infrared region. The higher energy band shows multiple structure on both its low and high energy sides. Absorption maxima and spectral parameters are listed in Table X and indicate that octahedral symmetry is closely approximated in $Co(H_2PO_2)_2$.

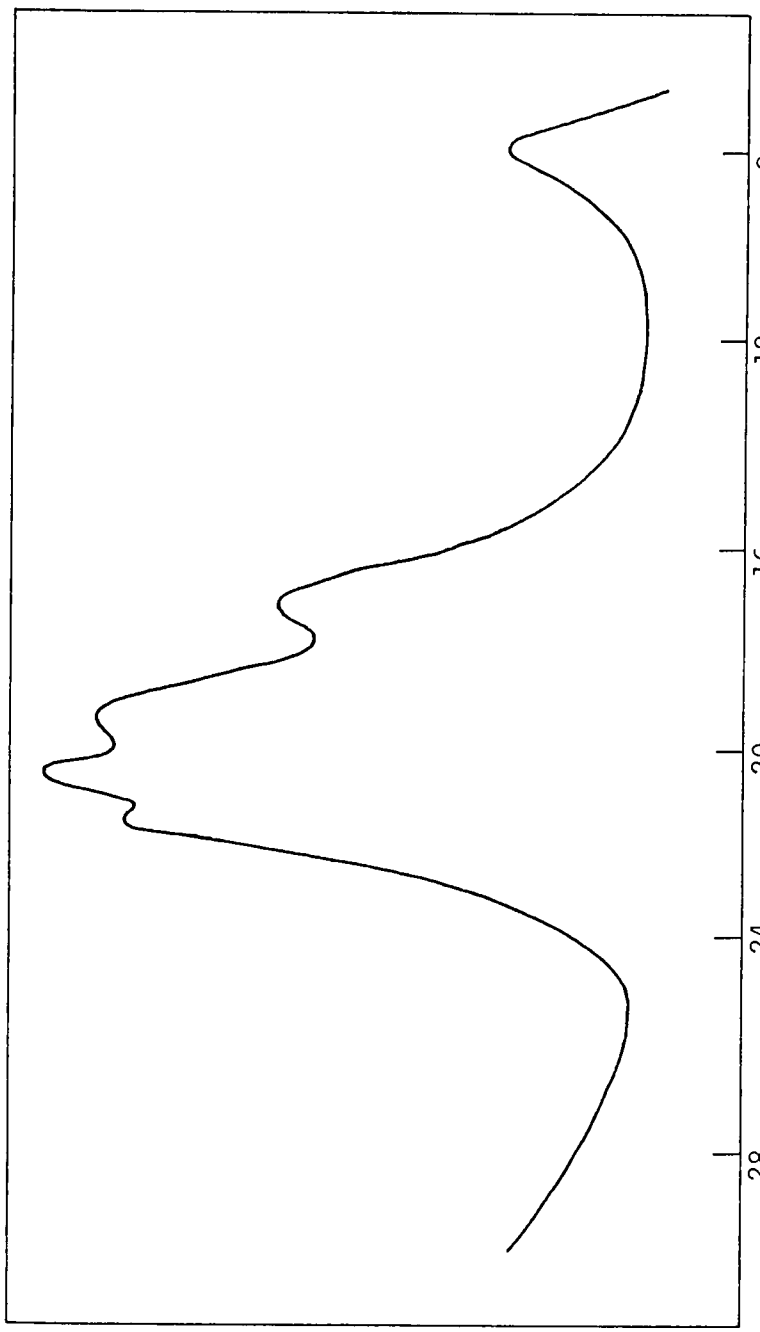

Figure 10. Visible and near-infrared spectrum of $Co(H_2PO_2)_2$ as a Nujol mull.

3. Nickel(II) Spectra

The nickel(II) ion has a $3d^8$ valence electron configuration which gives rise to a triplet ^3F ground state. In an octahedral crystal field the degeneracy of the ^3F term is removed and the $^3A_{2g}$ term corresponds to the ground state.

Three moderately intense spin-allowed transitions characterize the spectrum of the nickel(II) ion in a regular octahedral crystal field. In addition, weak spin-forbidden transitions to singlet levels are often observed. The spin-allowed bands generally have a gaussian-like shape with the second band (ν_2) sometimes splitting into a well-defined doublet.[52]

Deviations from octahedral symmetry can be caused by geometric distortions and/or nonidentical donor atoms. In a tetragonally distorted field arising from a decrease in field strength along the z axis, the orbital triplets $^3T_{1g}$ and $^3T_{2g}$ undergo further splitting; six spin-allowed transitions are permitted.[53] Figure 11 presents the correlation diagram for the nickel(II) ion in an octahedral field and in a tetragonally distorted octahedral field.

a. Methanesulfonate compounds. The visible and near-infrared spectra of $[Ni(py)_4(CH_3SO_3)_2]$ and $[Ni(4\text{-mepy})_4(CH_3SO_3)_2]$ are displayed in Figures 12 and 13, respectively. The mull spectra of both compounds are characterized by four main absorption areas. There is a very broad medium intensity band in the near-infrared region having a maximum at 8330 cm^{-1}. Near 11,500 and 13,500 cm^{-1} are found low intensity absorptions. The band near 16,500 cm^{-1} is rather intense and

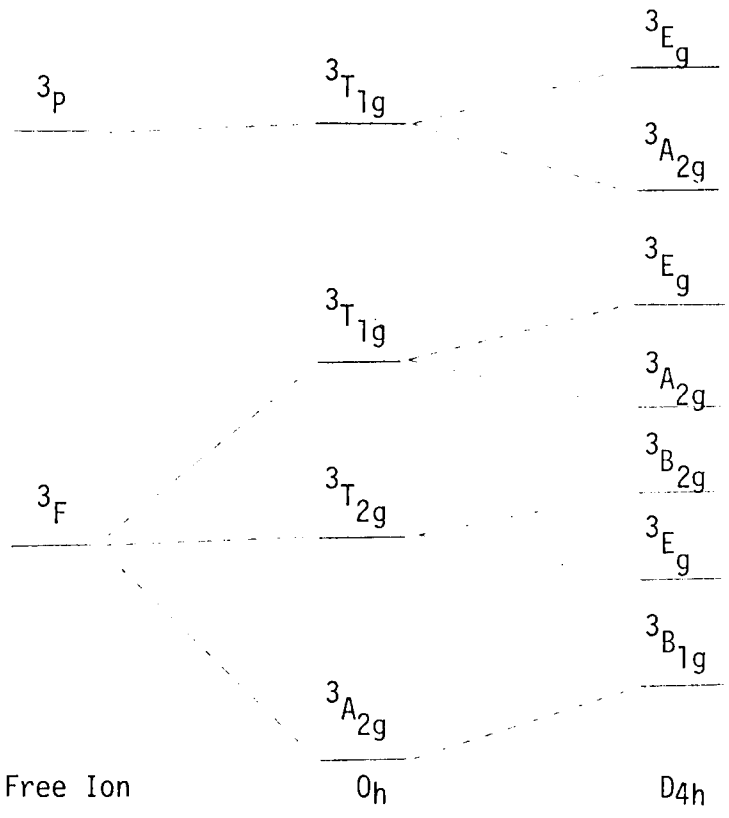

Figure 11. Correlation diagram for a d^8 configuration in crystal fields of O_h and D_{4h} symmetry.

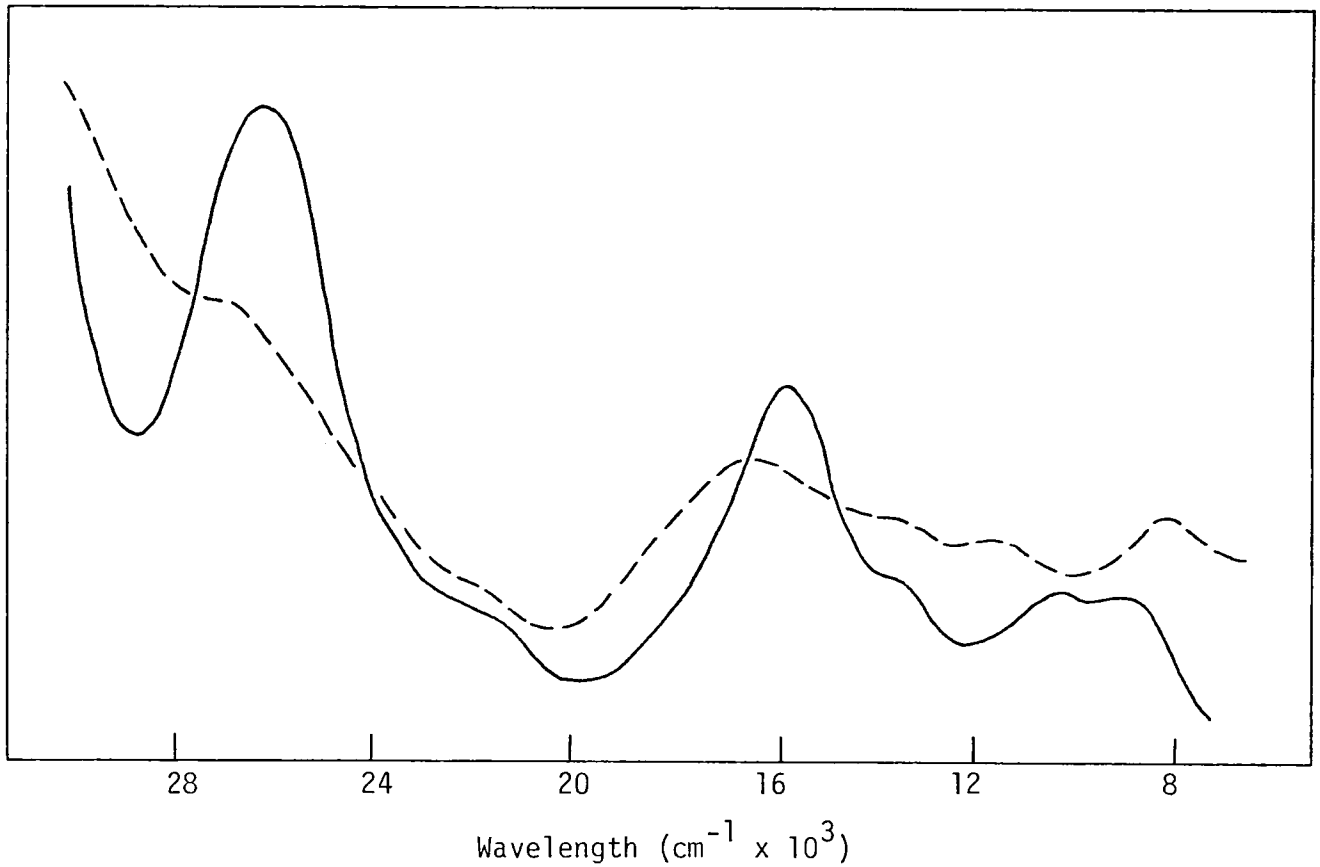

Figure 12. Visible and near-infrared spectra of $[Ni(py)_4(CH_3SO_3)_2]$ as a Nujol mull (dotted line) and as a dichloromethane solution (solid line).

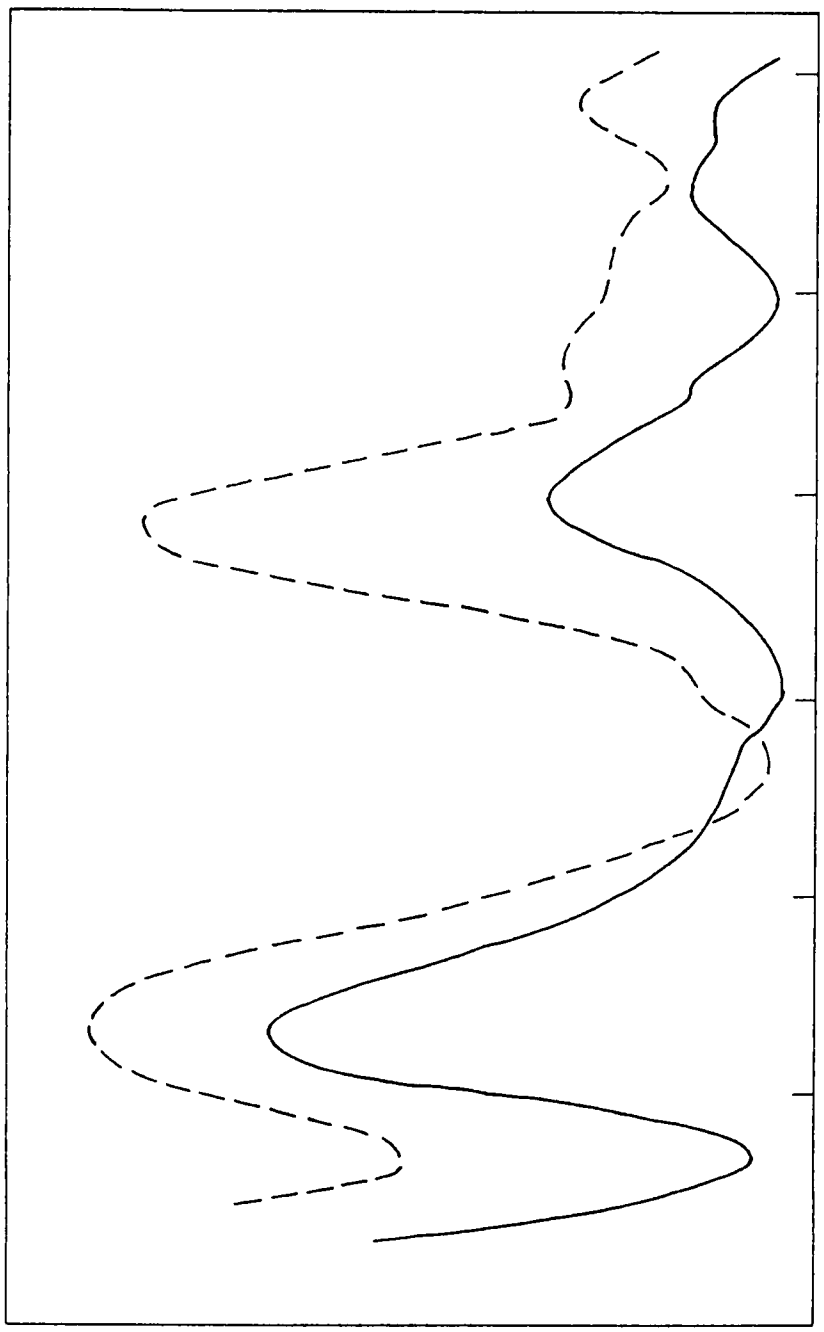

Figure 13. Visible and near-infrared spectra of $[Ni(4\text{-mepy})_4(CH_3SO_3)_2]$ as a Nujol mull (dotted line) and as a dichloromethane solution (solid line).

almost symmetrical. The highest intensity band has a maximum around 26,500 cm^{-1}. The visible and near-infrared spectral assignments are given in Table XI and are consistent with those in the literature for trans-$[NiL_4X_2]$ type complexes of approximately D_{4h} symmetry.[54]

From the close agreement of the positions of the absorption bands of the solid state and solution spectra, it is concluded that no significant decomposition has occurred on dissolution in dichloromethane.

Expressions relating the observed transition energies to the parameters Ds, Dt, Dq_{xy}, Dq_z and the Racah B' term have been developed for the nickel(II) ion[55] in a trans-$[NiL_4X_2]$ type complex. Ds and Dt are parameters which describe the splitting of the ^3F state while Dq_{xy} and Dq_z represent the ligand field strength in the xy-plane and along the z-axis, respectively.[53] Dt, Dq_{xy}, and Dq_z are related by the expression,

$$Dt = 4/7(Dq_{xy}-Dq_z).^{53} \qquad (4)$$

The value of the Racah parameter B' is an indication of the energy separation between the ^3F and ^3P levels.

Assignments for the two $^3B_{1g} \rightarrow {}^3A_{2g}$ transitions were calculated using equations for tetragonal d^8 configurations including configurational interaction between energy level terms of the same symmetry.[55] These equations and the relationship between the various terms are presented in the Appendix. Values for the three observed $^3B_{1g} \rightarrow {}^3E_g$ transitions along with that for $10Dq_{xy}$ (Δ_2) were substituted into the three by three determinant to solve for Δ_1, Δ_3, and B' using a least-squares computer program supplied by M. H. Lietzke and R. J. Herdklotz.

TABLE XI

ELECTRONIC SPECTRAL DATA FOR $[NiL_4(CH_3SO_3)_2]$ $(cm^{-1})^a$

Assignments	Absorption Maxima[b] L = py	L = 4-mepy
$^3B_{1g} \rightarrow {}^3E_g$	8330m	8330m
$^3B_{1g} \rightarrow {}^3B_{2g}$	11,900w	10,900w
$^3B_{1g} \rightarrow {}^3A_{2g}$	13,600w (14,240)[c]	13,300w (12,000)[c]
$^3B_{1g} \rightarrow {}^3E_g$	16,800s	16,000s
$^3B_{1g} \rightarrow {}^3A_{2g}$	21,700sh (25,640)[c]	20,400sh (23,200)[c]
$^3B_{1g} \rightarrow {}^3E_g$	27,000vs	26,300vs

[a]Nujol mull spectra.

[b]vs, Very strong; s, strong; m, medium; w, weak; sh, shoulder.

[c]Calculated values.

These values and $10Dq_{xy}$ were then used in the two by two determinant to solve for the $^3B_{1g} \rightarrow {}^3A_{2g}$ transitions. Δ_1, Δ_3, and B' values along with other calculated spectral parameters are presented in Table XI. The calculated values for the transitions do not fit the observed energies in all cases, particularly the higher energy transitions. The lack of agreement is due partly to the difficulty associated with estimating the position of a band maximum that appears as a shoulder on a more intense absorption. However, quite reasonable B' values (near 860) were obtained.

Expressions[56] which relate the crystal field parameters to molecular orbital parameters are given in the Appendix. These expressions apply only to high-spin trans-$[ML_4X_2]$ complexes. The quantity $d\sigma$, defined as $d\sigma = \sigma_z - \sigma_{xy}$, represents the difference in the sigma antibonding ability of ligands along the z-axis and the ligands in the xy-plane. A large positive $d\sigma$-value indicates strong σ-donor strength of the axial ligands when compared to the equatorial ligands. The quantity $d\pi$ represents the π-antibonding character and is defined as $d\pi = d\pi_z - d\pi_{xy}$. Thus, the quantities $d\sigma$ and $d\pi$ give a quantitative comparison of differences in bonding strength of the CH_3SO_3 group and the pyridine or 4-methylpyridine ligands.

Referring to Table XII, it is seen that in the nickel(II) compounds, the pyridine and 4-methylpyridine are stronger σ-donors than the methanesulfonate ion.

It is also evident from the sign of $d\pi$ that the π-antibonding interaction is greater in the xy-plane than along the z-axis.

Comparison of Dt values calculated from the electronic spectral data for various pyridine complexes[20,21] by the method presented in

TABLE XII

ELECTRONIC SPECTRAL PARAMETERS FOR $[NiL_4(CH_3SO_3)_2]$ (cm^{-1})

Parameter[a]	L = py	L = 4-mepy
Dq_{xy}	1190	1090
Dq_z	557	628
Ds	741	622
Dt	363	264
B'	862	867
Δ_1	355	547
Δ_2	11,900	10,900
Δ_3	4730	3809
$d\sigma$	- 1793	- 1428
$d\pi$	- 204	- 273

[a]All values include configurational interaction.

this thesis indicates that the methanesulfonate ion coordinates more strongly than the perchlorate (577 cm^{-1}), and the tetrafluoroborate (625 cm^{-1}), and less strongly than the chloride (307 cm^{-1}) and bromide (349 cm^{-1}) anions. The methanesulfonate ion has a Dt value very close to those for the perrhenate (368 cm^{-1}) and the trifluoromethanesulfonate (353 cm^{-1}) ions.

b. Hypophosphite compounds. The electronic spectrum of $Ni(H_2PO_2)_2$ is presented in Figure 14; no splitting of any of the spectral bands was observed and tetragonal distortion was concluded to be small. Accordingly, octahedral symmetry is assumed to be closely approximated and the three principal bands are assigned to the $^3A_{2g} \rightarrow {}^3T_{2g}$, $^3A_{2g} \rightarrow {}^3T_{1g}(F)$, and $^3A_{2g} \rightarrow {}^3T_{1g}(P)$ transitions. The moderately intense shoulder at 14,600 cm^{-1} has been assigned to the spin-forbidden $^3A_{2g} \rightarrow {}^1E_g({}^1D)$ transition which has gained intensity by configurational interaction with the $^3T_{1g}(F)$ level[57] or by spin-orbit coupling. A value of 930 cm^{-1} was calculated for the Racah parameter B' using the energy matrix for the $^3T_{1g}({}^3F)$ and $^3T_{1g}({}^3P)$ levels of Tanabe and Sugano:[58]

$$\begin{vmatrix} 6\,Dq - E & 4\,Dq \\ 4\,Dq & X - E \end{vmatrix} = 0 \qquad (5)$$

The energies of the $^3A_{2g}$ and $^3T_{2g}$ levels relative to the ^3F free ion state are -12 Dq and -2 Dq, respectively, with 10 Dq corresponding to the $^3A_{2g} \rightarrow {}^3T_{2g}$ transition. The nephelauxetic ratio, β, was determined to be 0.881.

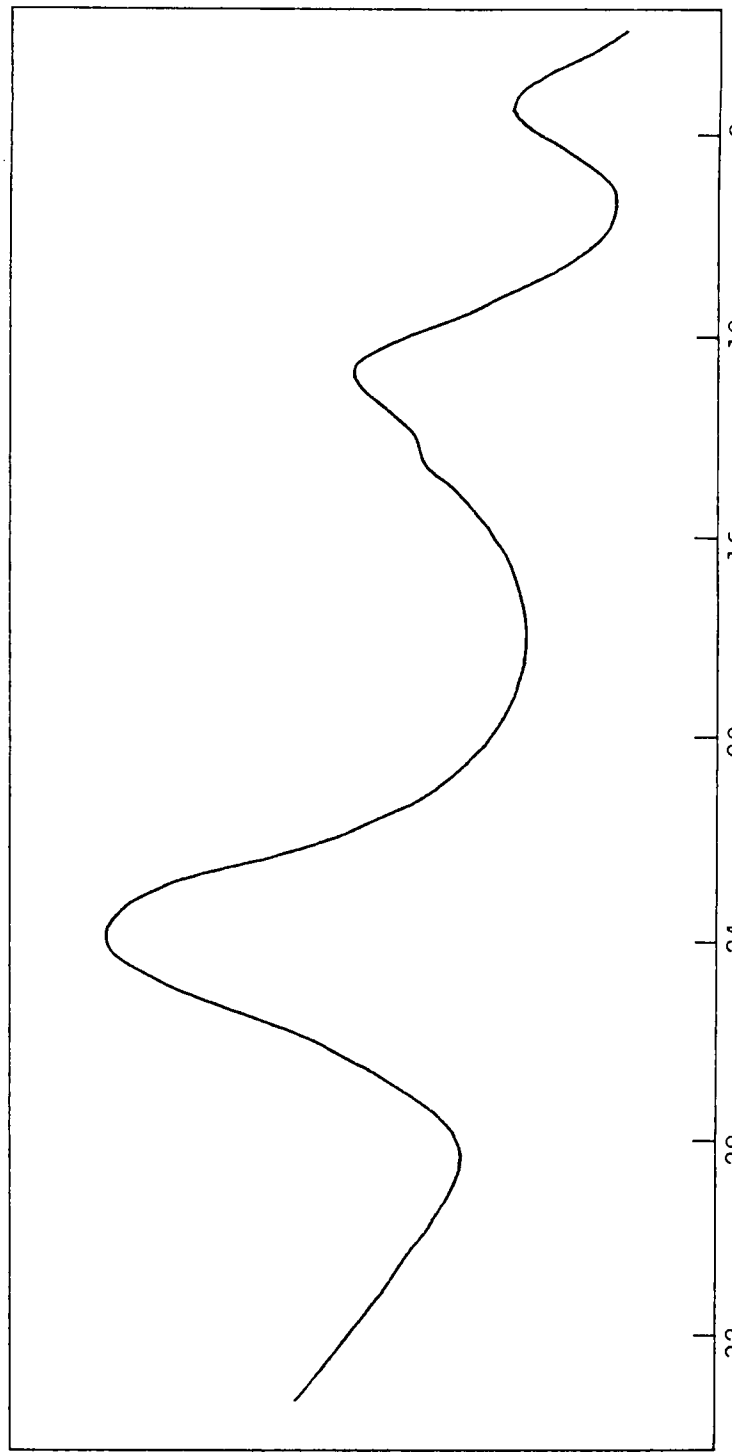

Figure 14. Visible and near-infrared spectrum of $Ni(H_2PO_2)_2$ as a Nujol mull.

From equation (5) an energy of 12,900 cm^{-1} was calculated for the $^3A_{2g} \rightarrow {}^3T_{1g}$ (^3F) transition. The agreement between observed and calculated values for this transition is good evidence for a regular octahedral structure. The electronic transitions, assignments, and parameters for the spectrum of $Ni(H_2PO_2)_2$ are listed in Table XIII and are consistent with those in the literature for regular octahedral nickel(II) complexes.[59]

$[Ni(py)_2(H_2PO_2)_2]$ absorbs strongly around 8620, 14,000, and 24,700 cm^{-1}. The spectrum of this complex closely approximates that of a regular octahedral structure; presumably the axial and the in-plane ligand field strengths are of comparable magnitude. Electronic transitions, assignments, and parameters for $[Ni(py)_2(H_2PO_2)_2]$ are listed in Table XIII; the electronic spectrum is presented in Figure 15. Absorptions at 14,700 and 19,800 cm^{-1} are assigned to spin-forbidden transitions to singlet levels derived from ^1D and ^1G free ion terms.[57]

4. Copper(II) Spectra

The free copper(II) ion has a d^9 configuration giving rise to the ^2D ground spectroscopic state. When placed in an octahedral environment, the ^2D level splits into a lower energy ^2E_g component and a higher energy $^2T_{2g}$ component. Thus, the electronic spectrum of a copper(II) ion in an octahedral field should consist of a single transition. Jahn-Teller effects, spin-orbit coupling, or ligand in equivalencies, however, often produce additional bands or shoulders on the main band.[60] If tetragonal perturbation of the octahedral field occurs by decreasing the ligand field strength along the z axis, the energy levels would be further split. Three spin-allowed transitions are expected for D_{4h}

TABLE XIII

ELECTRONIC SPECTRAL DATA FOR $Ni(H_2PO_2)_2$ AND $[Ni(py)_2(H_2PO_2)_2]$

Assignment or Parameter	Absorption Maxima (cm^{-1})[a] $Ni(H_2PO_2)_2$	$[Ni(py)_2(H_2PO_2)_2]$
$^3A_{2g} \rightarrow {}^3T_{2g}$	7690m	8620s
$^3A_{2g} \rightarrow {}^3T_{1g}(^3F)$	12,800s (12,900)[b]	13,500s (14,100)[b]
$^3A_{2g} \rightarrow {}^1E_g(^1D)$	14,600sh	14,700s
$^3A_{2g} \rightarrow {}^1T_{2g}(^1D)$, $^1A_{1g}(^1G)$		19,800w
$^3A_{2g} \rightarrow {}^3T_{1g}(^3P)$	24,100vs	24,700vs
10Dq	7690	6820
B'	930	825
β	0.881	0.781

[a] vs, Very strong; s, strong; w, weak; sh, shoulder.

[b] Calculated values.

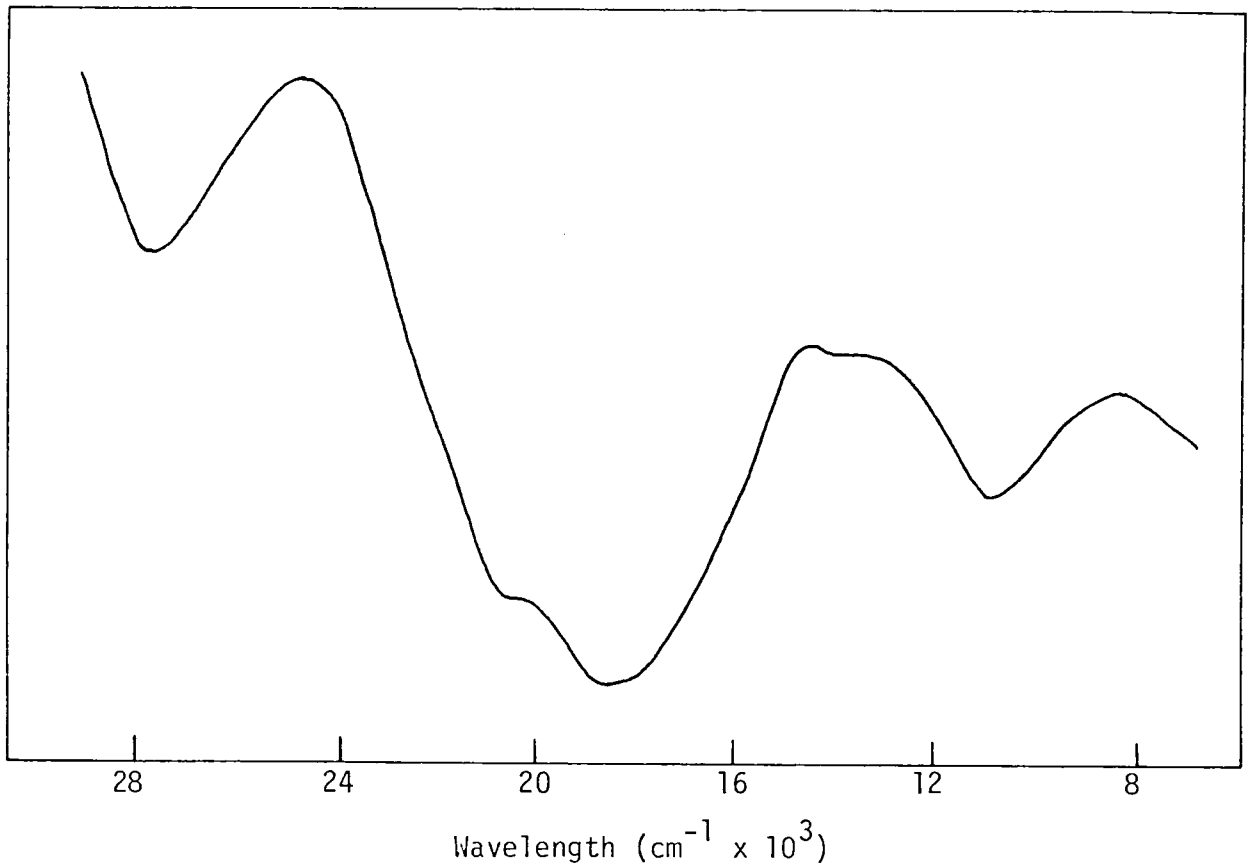

Figure 15. Visible and near-infrared spectrum of $[Ni(py)_2(H_2PO_2)_2]$ as a Nujol mull.

symmetry; however, the precise order of the energy levels in this symmetry is uncertain and may vary with the extent of metal axial-ligand interaction.[61] The ordering presented in Figure 16 has been suggested for low tetragonal distortion. The $^2B_{1g} \rightarrow {}^2E_g$ transition is likely to correspond to the most intense absorption.[61]

Table XIV contains the electronic absorption bands for $[Cu(py)_4(CH_3SO_3)_2]$ and for $[Cu(4\text{-mepy})_4(CH_3SO_3)_2]$ in dichloromethane solution and as Nujol mulls. The spectra of the 4-methylpyridine complex are presented in Figure 17. The shift of the absorption band to lower frequency in nonpolar dichloromethane indicates that the weakly-coordinating methanesulfonate anion is probably liberated in solution.

For both complexes, absorption in the visible and near-infrared regions (as Nujol mulls) consists of a single almost symmetrical broad band of maximum intensity near 17,000 cm^{-1} which tails into the near-infrared. This band position is indicative of tetragonally distorted octahedral complexes. Since only one region of absorption attributable to d-d transitions is observed, all three transitions probably occur under the broad band envelope.

It has been suggested[20,62] that the energy of the visible band maximum provides a measure of the degree of tetragonal distortion in copper(II) complexes. Based upon the data in Table XIV, the degree of tetragonal distortion in $[Cu(py)_4(CH_3SO_3)_2]$ appears to be less than that of the nitrate and tetrafluoroborate complexes but slightly greater than the corresponding fluorosulfate complex.

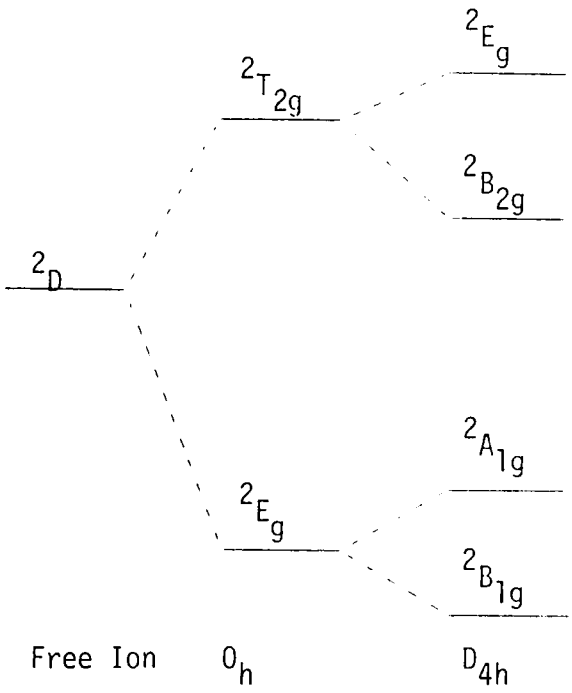

Figure 16. Splitting of the ^2D spectroscopic term for copper(II) in octahedral and tetragonally distorted octahedral fields.

TABLE XIV

ELECTRONIC ABSORPTION BANDS FOR
COPPER(II) COMPLEXES

Compound	Absorption Maxima (cm^{-1})[a] Mull	Solution
$[Cu(py)_4(CH_3SO_3)_2]$	17,900s	13,700s
$[Cu(4\text{-mepy})_4(CH_3SO_3)_2]$	17,000s	14,400s
$[Cu(py)_4(NO_3)_2]$[b]	18,300	
$[Cu(py)_4(BF_4)_2]$[b]	18,000	
$[Cu(py)_4(SO_3F)_2]$[b]	17,200	

[a] s, Strong.

[b] Source: C. S. Alleyne and R. C. Thompson, Can. J. Chem., 52, 3218 (1974).

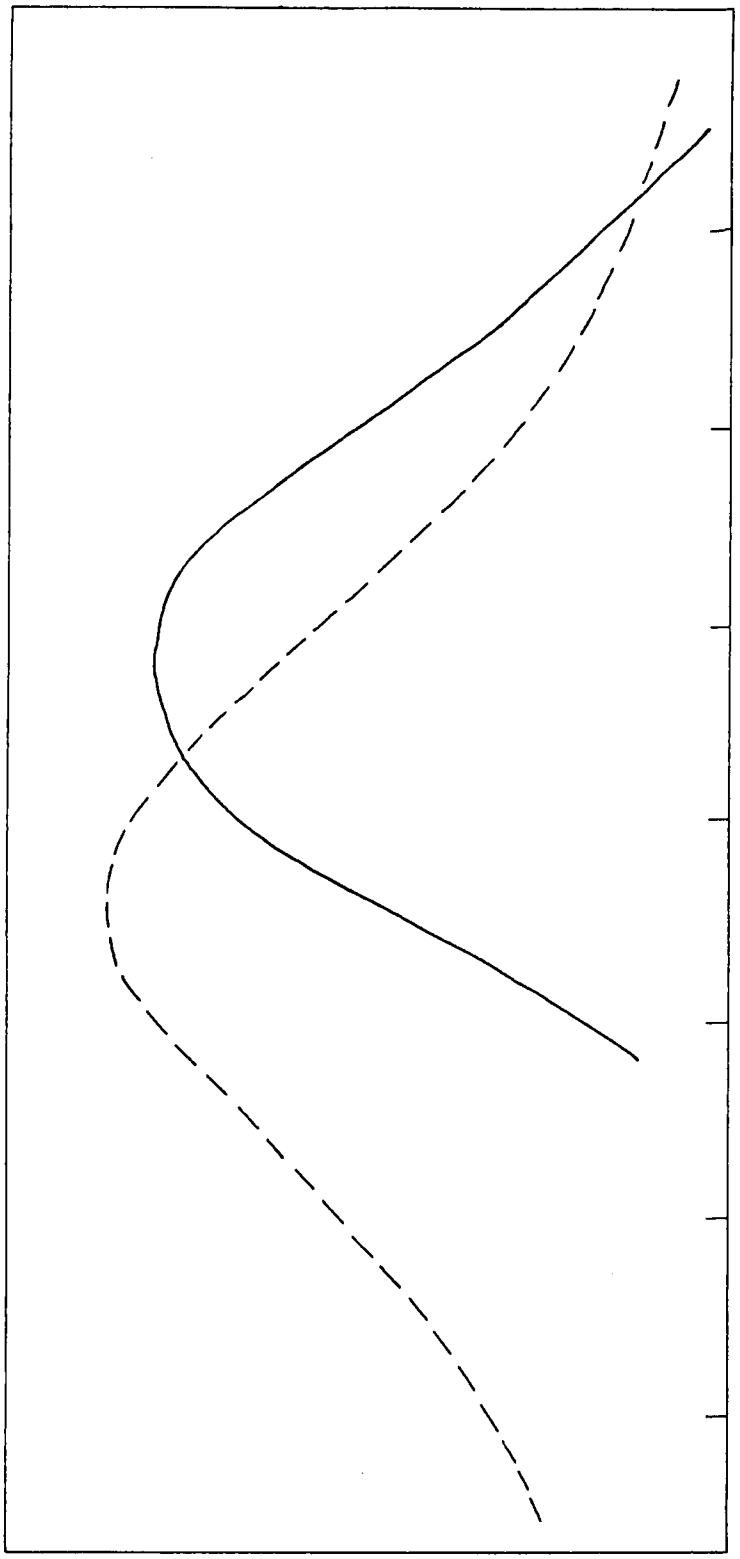

Figure 17. Visible and near-infrared spectra of $[Cu(4\text{-mepy})_4(CH_3SO_3)_2]$ as a Nujol mull (dotted line) and as a dichloromethane solution (solid line).

CHAPTER IV

SUMMARY

Two series of compounds were prepared. The first has the general formula $[ML_4(CH_3SO_3)_2]$ where M represents Co(II), Ni(II), and Cu(II) and L represents pyridine and 4-methylpyridine. The second series contains anhydrous $Co(H_2PO_2)_2$ and $Ni(H_2PO_2)_2$. Also prepared were $[Co(py)_2(CH_3SO_3)_2]$ and $[Ni(py)_2(CH_3SO_3)_2]$.

Magnetic susceptibility measurements indicate that the cobalt(II) and nickel(II) compounds are high-spin octahedral type complexes.

Anion coordination was ascertained using middle and far-infrared data. Monodentate coordination is indicated in the $[ML_4(CH_3SO_3)_2]$ complexes. Bidentate coordination as bridging and chelating ligands is suggested for $Co(H_2PO_2)_2$, $Ni(H_2PO_2)_2$, $[Co(py)_2(H_2PO_2)_2]$, and $[Ni(py)_2(H_2PO_2)_2]$.

Electronic spectroscopy of the $[ML_4(CH_3SO_3)_2]$ complexes is indicative of tetragonally distorted octahedral structures consistent with D_{4h} symmetry. The electronic spectra of the cobalt complexes give further support of a trans arrangement of the methanesulfonate anions.

Electronic spectra for the nearly anhydrous hypophosphites and for $[Co(py)_2(CH_3SO_3)_2]$ and $[Ni(py)_2(H_2PO_2)_2]$ suggest the close approximation of octahedral symmetry.

Crystal field splitting parameters, Ds and Dt, were calculated for the $[NiL_4(CH_3SO_3)_2]$ complexes. The coordination strength of the methanesulfonate anion was compared with that of other anions of strong

acids. It was found that the methanesulfonate anion coordinates less strongly than Cl^- and Br^-, but more strongly than ClO_4^- and BF_4^-. The value of Dt for $CH_3SO_3^-$ is very similar to the reported values for ReO_4^- and $CF_3SO_3^-$.

LIST OF REFERENCES

LIST OF REFERENCES

1. K. N. Bascombe and R. P. Bell, J. Chem. Soc., 1096 (1959).

2. E. A. Robinson, Can. J. Chem., 39, 247 (1961).

3. J. Bessiere, Bull. Soc. Chim. Fr., 9, 3356 (1969).

4. T. A. Modro, K. Yates, and J. Janata, J. Am. Chem. Soc., 97, 1492 (1975).

5. R. C. Paul, V. P. Kapila, N. Palta, and S. K. Sharma, Indian J. Chem., 12, 825 (1974).

6. P. A. Yeats, J. R. Sams, and F. Aubke, Inorg. Chem., 10, 1877 (1971).

7. A. Simon, H. Kriegsmann, and H. Dutz, Chem. Ber., 89, 2378 (1956).

8. H. Gerding and J. W. Maarsen, Rec. Trav. Chim. Pays-Bas., 77, 374 (1958).

9. K. Fujimori, Bull. Chem. Soc. Japan, 32, 850 (1959).

10. R. J. Gillespie and E. A. Robinson, Can. J. Chem., 40, 644 (1962).

11. S. M. Chackalackal and F. E. Stafford, J. Am. Chem. Soc., 88, 4815 (1966).

12. A. Nersasian and P. R. Johnson, J. Appl. Polym. Sci., 9, 1653 (1965).

13. R. J. Capwell, K. H. Rhee, and K. S. Seshadri, Spectrochim. Acta, 24A, 955 (1968).

14. K. Fujimori, Bull. Chem. Soc. Japan, 32, 621 (1959).

15. L. E. Moore, Ph.D. Dissertation, The University of Tennessee, Knoxville, Tennessee, 1964; W. E. Bull and L. E. Moore, J. Inorg. Nucl. Chem., 27, 1341 (1965); L. E. Moore, R. B. Gayhart, and W. E. Bull, J. Inorg. Nucl. Chem., 26, 897 (1964).

16. W. C. Jones, Ph.D. Dissertation, The University of Tennessee, Knoxville, Tennessee, 1966; W. C. Jones and W. E. Bull, J. Chem. Soc., Sect. A 1849 (1968).

17. D. H. Brown, R. N. Nuttall, J. McAvoy, and D. W. A. Sharp, J. Chem. Soc., Sec. A, 892 (1966).

18. M. R. Rosenthal and R. S. Drago, Inorg. Chem., 4, 840 (1965).

19. S. Buffagni, L. M. Vallarino, and J. V. Quagliano, Inorg. Chem., 3, 671 (1964).

20. H. G. Mayfield, Jr., Ph.D. Dissertation, The University of Tennessee, Knoxville, Tennessee, 1970; H. G. Mayfield and W. E. Bull, J. Chem. Soc., Sect. A, 2279 (1971).

21. A. R. Byington, M.S. Thesis, The University of Tennessee, Knoxville, Tennessee, 1973; A. R. Byington and W. E. Bull, submitted for publication in Inorg. Chim. Acta.

22. M. R. Rosenthal, J. Chem. Educ., 50, 331 (1973).

23. J. T. Turk, H. G. Mayfield, and W. E. Bull, unpublished results.

24. Chem. Abstr., 51, 14458d (1957); [R. A. Paris and J. C. Merlin, Silicium, Schwefel, Phosphate, Colloq. Sek. Anorg. Chem. Intern. Union Reine u. Angew. Chem. Munster, 237 (1954)].

25. G. Brun and M. Dumail, Compt. Rend., 272, 1866 (1971).

26. R. W. Lovejoy and E. L. Wagner, J. Phys. Chem., 68, 544 (1964).

27. W. H. Zachariasen and R. C. L. Mooney, J. Chem. Phys., 2, 34 (1934).

28. J. S. Ziomek, J. R. Ferraro, and D. F. Peppard, J. Mol. Spectrosc., 8, 212 (1962).

29. M. Tsuboi, J. Am. Chem. Soc., 79, 1351 (1957).

30. L. S. Mayants and E. I. Matrosov, Izv. Akad. Nauk SSSR, Neorg. Mater., 1, 546 (1965).

31. J. P. Mathieu and J. Jacques, Compt. Rend., 215, 346 (1942).

32. D. E. C. Corbridge and E. J. Lowe, J. Chem. Soc., 493 (1954).

33. C. Duval and J. Lecomte, Compt. Rend., 240, 67 (1955).

34. H. Gerding, J. W. Maarsen, and D. H. Zijp, Rec. Trav. Chim. Pays-Bas., 77, 361 (1958).

35. W. A. Jenkins and R. T. Jones, J. Am. Chem. Soc., 74, 1353 (1952).

36. R. T. Jones and E. H. Swift, Anal. Chem., 25, 1272 (1953).

37. K. Starke, J. Inorg. Nucl. Chem., 11, 77 (1959).

38. C. S. Alleyne, K. O. Mailer, and R. C. Thompson, Can. J. Chem., 52, 337 (1974).

39. B. N. Figgis and R. S. Nyholm, J. Chem. Soc., 4190 (1958).

40. B. N. Figgis and J. Lewis in "Modern Coordination Chemistry," J. Lewis and R. G. Wilkins, Eds., Interscience Publishers, Inc., New York, N. Y., 1960, p. 403.

41. T. H. Tan, J. R. Dalziel, P. A. Yeats, J. R. Sams, R. C. Thompson, and F. Aubke, Can. J. Chem., 50, 1843 (1972).

42. J. G. David and H. E. Hallam, J. Chem. Soc., Sect. A, 1103 (1966).

43. N. S. Gill, R. H. Nuttall, D. E. Scaife, and D. W. A. Sharp, J. Inorg. Nucl. Chem., 18, 79 (1961).

44. R. J. H. Clark and C. S. Williams, Inorg. Chem., 4, 350 (1965).

45. F. A. Cotton and G. W. Wilkinson, "Advanced Inorganic Chemistry," 3rd ed., Interscience Publishers, New York, N. Y., 1972, p. 560.

46. C. J. Ballhausen and C. K. Jorgensen, Acta Chem. Scand., 9, 397 (1955).

47. A. B. P. Lever, "Inorganic Electronic Spectroscopy," Elsevier Publishing Company, New York, N. Y., 1966, p. 318.

48. S. Koide, Phil. Mag., 4, 243 (1959).

49. J. A. Kakazal and G. A. Melson, Inorg. Chim. Acta, 4, 360 (1970).

50. C. J. Ballhausen, "Introduction to Ligand Field Theory," McGraw-Hill, New York, 1962, p. 256.

51. A. B. P. Lever, "Inorganic Electronic Spectroscopy," Elsevier Publishing Company, New York, N. Y., 1966, p. 209.

52. L. Sacconi in "Transition Metal Chemistry," Vol. 4, R. L. Carlin, Ed., Marcel Dekker, Inc., New York, N. Y., 1968, pp. 211-2.

53. A. B. P. Lever, Coordin. Chem. Rev., 3, 119 (1968).

54. D. A. Rowley and R. S. Drago, Inorg. Chem., 7, 795 (1968).

55. A. B. P. Lever, "Inorganic Electronic Spectroscopy," Elsevier Publishing Company, New York, N. Y., 1966, pp. 193 and 409.

56. D. S. McClure in "Advances in the Chemistry of Coordination Compounds," S. Kirshner, Ed., The Macmillan Co., New York, N. Y., 1961, p. 498.

57. H. G. Mayfield, Jr., Ph.D. Dissertation, The University of Tennessee, Knoxville, Tennessee, 1970, pp. 59 and 67.

58. Y. Tanabe and S. Sugano, J. Phys. Soc. Japan, 9, 753 (1954).

59. A. B. P. Lever, "Inorganic Electronic Spectroscopy," Elsevier Publishing Company, New York, N. Y., 1966, pp. 334-6.

60. H. Elliott and B. J. Hathaway, Inorg. Chem., 5, 885 (1966).

61. I. M. Procter, B. J. Hathaway, and P. Nicholls, J. Chem. Soc., Sect. A, 1678 (1968).

62. C. S. Alleyne and R. C. Thompson, Can. J. Chem., 52, 3218 (1974).

APPENDIX

APPENDIX

ENERGY LEVEL RELATIONS FOR TETRAGONAL NICKEL(II) COMPLEXES

The energies of the six spin-allowed electronic transitions relative to the $^3B_{1g}$ ground level as zero and inclusive of configurational interaction between the three E_g levels and between the two A_{2g} levels are given by Equations 6, 7, and 8.[55]

$$^3B_{1g} \rightarrow {}^3B_{2g} = \Delta_2 \tag{6}$$

A_{2g}^a, A_{2g}^b

$$\begin{vmatrix} \Delta_2 - \Delta_3 + 12B - E & 6B \\ 6B & 2\Delta_1 + 2\Delta_2 - \Delta_3 + 3B - E \end{vmatrix} = 0 \tag{7}$$

E_g^a, E_g^b, E_g^c

$$\begin{vmatrix} \Delta_1 + \Delta_2 - \Delta_3 + 3B - E & -3B & \\ +3\sqrt{3}\,B & \Delta_1 + \Delta_2 + 9B - E & -3\sqrt{3}\,B \\ -3B & -3\sqrt{3}\,B & \Delta_1 + 2\Delta_2 - \Delta_3 + 3B - E \end{vmatrix} = 0 \tag{8}$$

In these equations, Δ_1, Δ_2, and Δ_3 correspond to the energy separation of the d orbitals as shown in Figure 18. The relations linking Δ_1, Δ_2, and Δ_3 to Dq_{xy}, Ds, and Dt are presented in Equation 9.

$$\Delta_1 = 3Ds - 5Dt$$
$$\Delta_2 = 10Dq_{xy}$$
$$\Delta_3 = 4Ds + 5Dt$$

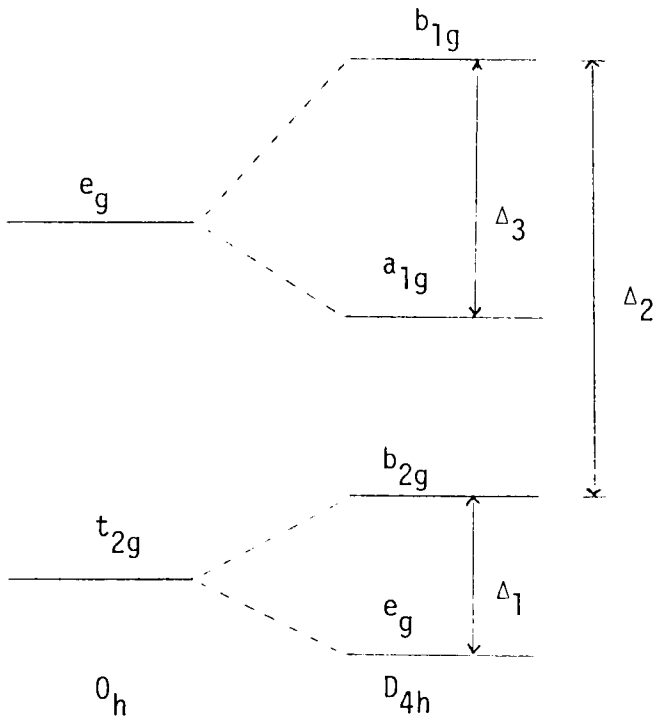

Figure 18. Splitting of the d orbitals in crystal fields of O_h and D_{4h} symmetry.

Finally, the relationships[56] between the crystal field parameters Ds and Dt and McClure's molecular orbital parameters are presented in Equation 10.

$$8d\sigma = -12Ds - 15Dt$$
$$2d\pi = -3Ds + 5Dt \qquad (10)$$

VITA

Nancy Lee Copeland Johnson was born in Suffolk, Virginia, on July 9, 1952. She attended the public schools of that city and was graduated from Forest Glen High School in June 1970. She then entered Lynchburg College and received the Bachelor of Science degree in May 1974.

In September 1974 she entered the Graduate School of the University of Tennessee where she held a teaching assistantship for two years.

Mrs. Johnson is a member of the American Chemical Society. She is presently employed by the Naval Surface Weapons Center of White Oak, Maryland.